RUTTER

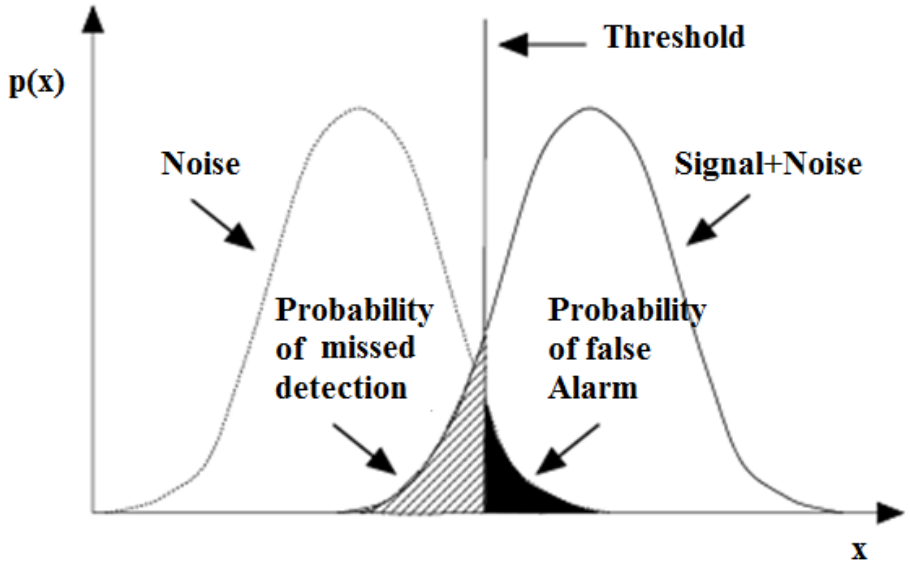

Probability of detection = area under the signal +noise curve above threshold

Radar Data Collection Trial Analysis Report

12 July 2011

Contents

1 Introduction

Rutter Inc. undertook a large data collection program to record, collect, and analyze radar data of fast rescue craft (FRC), Person in Water (PIW), Helicopter (HELO) flight path approach and sea clutter at various sea states. The two main goals of this project are to enhance Rutter's understanding of the theoretical detection performance of radar when augmented with special features and to collect full bandwidth high fidelity raw radar data recordings that can be used to design and validate future product developments.

During this project two large field trials were undertaken. The first trial took place during the week of March 8th 2010 in Placentia Bay, Newfoundland at the Argentia military airbase site. During this weeklong trial fast rescue craft (FRC) and Persons in Water (PIW) radar data was collected. The second trial took place during the months of December and January 2011 just outside of St. John's Harbor at the "Skerries" site, and at a second site off of Cape Spear. During this trial FRC, PIW, helicopter (HELO) approach, and sea clutter data recordings were collected.

During the first Argentia trial the radar equipment used did not have all the features that were required for a complete analysis and also the vertically polarized radar antenna that was being used was an older prototype that caused issues in our analysis. Therefore, the major portion of the discussion and analysis is performed on the data from the second Skerries/Cape Spear trial data as seen in Section 3 of this document. The Argentia data is also analyzed to a lesser extent in Section 2.

In order to enable a direct comparison of the radar data collected by the different radar systems and configurations being used throughout this project all the radars had to be calibrated. The calibration was performed on March 10, 2011 and the results are presented in Appendix A.

1.1 Data Analysis

This report discusses and presents the results from the analysis of the FRC, PIW and HELO data. The analysis provides performance data on the detection of these various targets as a function of range, sea state and radar parameters (antenna speed, pulse length, and vertical / horizontal antenna polarization).

The specific radar and target features being compared in this report are as follows:

- Comparison of a vertically polarized radar antenna vs. a horizontally polarized antenna for detection of FRC and PIW targets.
- Comparison of scan averaging vs. no scan averaging for detection of FRC and PIW targets.
- Comparison of radar rotation rate (RPM) for detection of moving FRC targets.
- Determine maximum detection range for the helicopter target.

The performance of a radar system is usually evaluated by the ability to distinguish the reflected target signal from sea clutter and system noise. Since the target signal is mixed with noise and sea clutter, radar signal detection is probabilistic in nature. Therefore this type of performance is quantitatively defined by Probability of Detection (P_d) and Probability of False Alarm (P_{fa}). Calculation of the P_d and P_{fa} are therefore the main means of doing radar target detection

performance comparisons in this report. The next section describes a method for obtaining the P_d and P_{fa} from the recorded radar data.

1.2 Calculation of P_d and P_{fa}

The probability of detecting a radar target against the background noise and clutter is called the Probability of Detection (P_d), and the probability that the reflected clutter or noise signal is mistaken as a target is called the Probability of False Alarm (P_{fa}). P_d is a function of P_{fa} and should be affected by the target size, sea state, amount of scan averaging, target range, target speed, and radar pulse length.

In order to calculate P_d and P_{fa} from the recorded radar data, two zones are set up: target zones and clutter zones. The target zone is an area containing the target and it is chosen to be as small as possible. The clutter zone includes an area much bigger than the target zone. Fig. 1 shows an example of a B-scan radar image containing the clutter and target zones. The red circle inside the target zone indicates a target hit, and the red circles inside the clutter zone indicate the clutter hits.

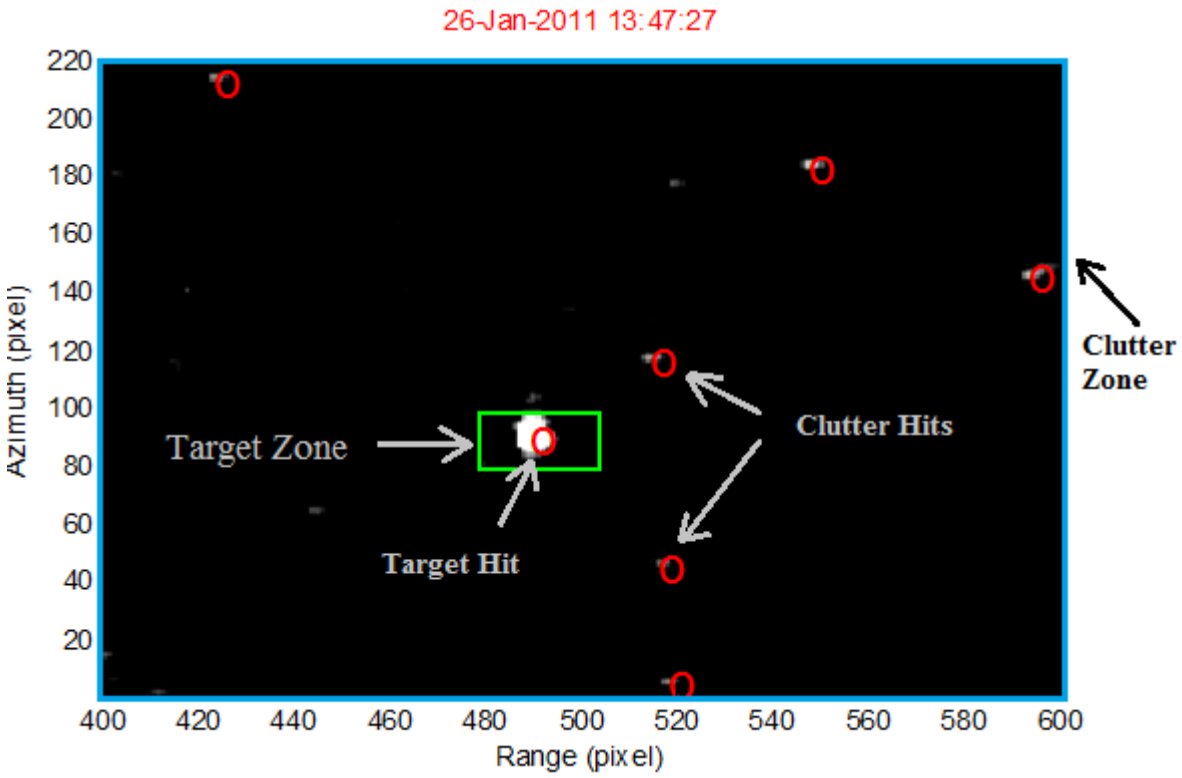

Figure 1: Clutter and target zones on a B-scan radar image. The radar image blobs are detected by Sigma S6 plot extractor. The blob inside the target zone is counted as a target hit, and the blobs inside the clutter zone are counted as clutter hits.

The probability of false alarm is calculated using the following formula:

$$P_{fa} = \frac{\text{clutter hits - targets hits}}{\text{clutter opp. - target opp.}} \times 100\% \quad (1)$$

where

$$\text{clutter opp.} = \text{number of clutter cells} \times \text{number of scans} \quad (2)$$

$$\text{target opp.} = \text{number of target cells} \times \text{number of scans} \quad (3)$$

The number of clutter cells is the number of pixels inside the clutter zone area divided by the number of pixels inside a radar resolution cell. The radar resolution cell area (in B-scan domain) is:

$$\text{resolution cell} = \frac{c\tau\theta}{2} \quad (4)$$

where c is the speed of light (3e8 m/s), τ is the pulse length (seconds), and θ (radians) is the antenna beam width. Similarly, the number of target cells is the number of pixels inside the target zone divided by the number of pixels inside a resolution cell.

For the P_{fa} calculated in (1), the probability of detection is obtained using the following formula:

$$P_d = [\text{target\_hits} - (P_{fa} * \text{target\_opp.})] \ / \ \text{number\_of\_scans} \quad (5)$$

The precision of the P_d calculation is inversely proportional to the number of scans used in the P_d calculation. For example, when the P_d is calculated over 100 scans, the precision will be 1%. In order to calculate P_{fa} and P_d with sufficient precision for this radar data, a minimum of two minutes of recording is needed.

In order to have an equivalent comparison of the P_d of a target under various conditions, the P_{fa} for all the measurements must be equal. Because of this, calculating the P_d and P_{fa} of a target is an iterative process. First, a threshold value is chosen. Second, P_{fa} and P_d are calculated by counting all the clutter and target hits for all the scans. If the calculated P_{fa} is not in the desired range ($10^{-4}<P_{fa}<10^{-6}$), the threshold is changed and the blobs are counted again for all the scans until the desired P_{fa} is obtained. The analysis usually requires changing the threshold and processing the data multiple times to obtain the desired P_{fa}.

2 Argentia Data Analysis

The Argentia Trial was the first trial performed for this project and took place during the week of March 8th 2010 in Placentia Bay, Newfoundland at the Argentia military airbase site. During this weeklong trial FRC and PIW radar target data was collected.

To determine sea states a preexisting wave buoy in the Argentia area was used. It is a wave buoy deployed by "Smart Bay" at the "Pilot Boarding Station / Red Island Shoal" location (Lat 47° 19.2759' N, Lon 054° 07.8118' W). The buoy was approximately 5.3 Nm off shore so it wasn't in the exact location of our trial but it was close enough to give an approximation of the local sea state.

The radar transceivers used during the Argentia trial were both made by Sperry. One of the systems used an 8ft vertically polarized antenna prototype (P13). The second system used an off-the-shelf 8ft horizontally polarized Sperry antenna (H1). Since both radars were only capable of rotation speeds of 24 and 48 RPM, high speed radar data (60, 80 and 120 RPM) was unable to be collected during this trial. Also, the vertically polarized (VPOL) radar antenna that was used was an older prototype that had high side lobe levels of approx. -22 dB. Standard marine radar antennas should have side lobe levels below -30 dB. These high side lobes caused false targets from the surrounding land to be projected onto the trial area. This caused issues with calculation of P_d and P_{fa} in the VPOL radar data. For these reasons the Argentia data is only partially useful for the goals of this analysis.

2.1 Person in Water (PIW)

The Argentia PIW data was collected on March 11th and 12th, 2010. Both radars were working simultaneously. The estimated sea states on March 11th and March 12th were 3 and 1, respectively.

The analysis of the VPOL data was affected by the high antenna side-lobe level. Fig. 8 shows an example of an image that clearly shows the effects of the high side lobe level. The false returns add to the clutter which in turn lowers the P_d value (for the same P_{fa} value). Since the VPOL data was affected by the false side lobe returns comparisons of HPOL vs VPOL target detection performance cannot be made.

The results of the P_d analysis of the PIW data are shown in Tables XII-XVII. In all cases, we see that scan averaging improves the radar performance significantly. It is inconclusive how the antenna rotation speed affects the P_d value. We see different P_d values for different rotations speeds but in some cases the P_d value increases and in others it decreases. This is most likely due to the fact that the different rotation speeds are recorded at different times and therefore there will be slightly different clutter conditions. It is expected that radar rotation rate should not affect probability of detection in this case since the PIW is a stationary target. As expected, for most cases, the P_d value of the VPOL data is less than the equivalent HPOL data due to the false side lobe returns.

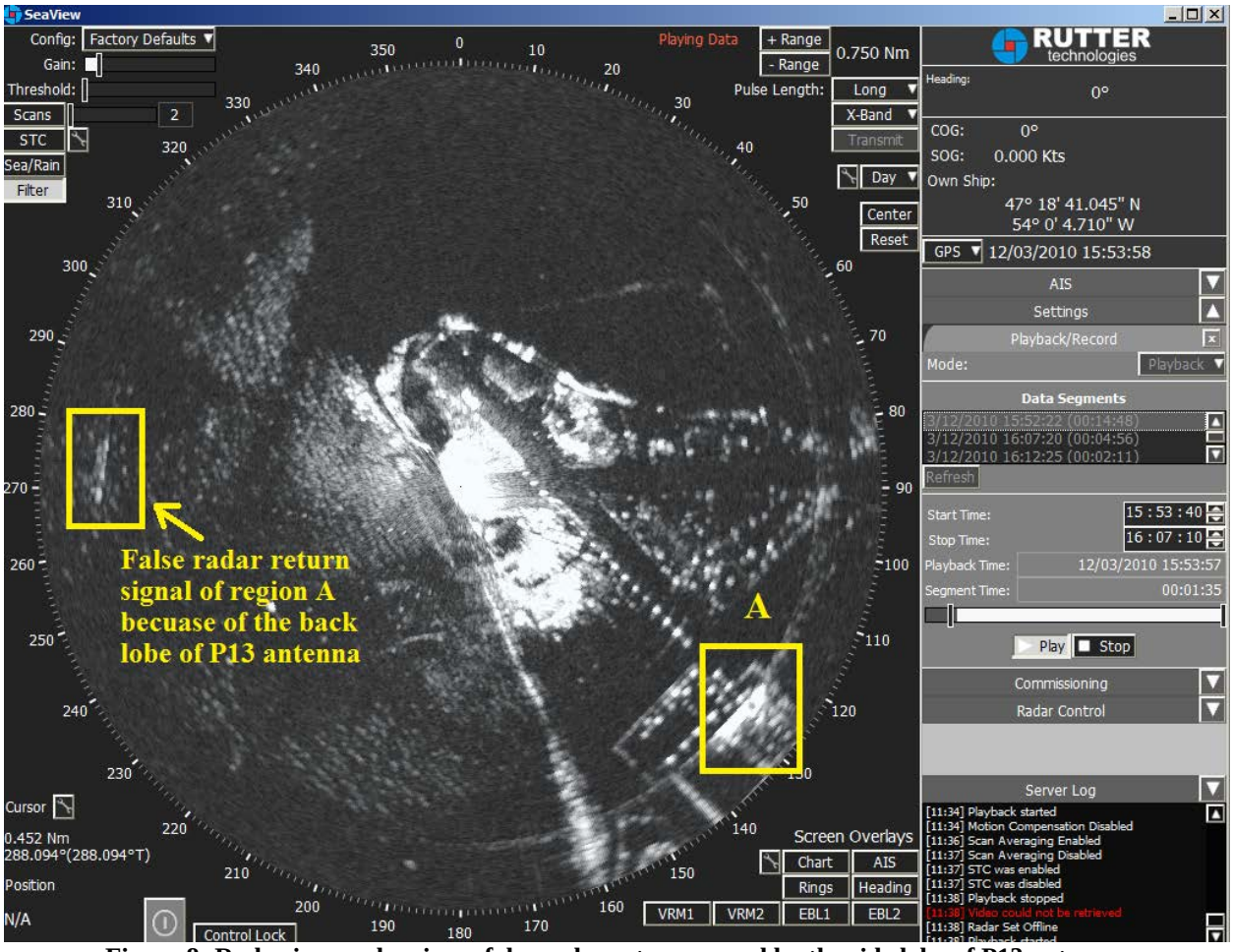

Figure 8: Radar image showing a false radar return caused by the side lobe of P13 antenna.

Table XII: P_{fa} and P_d calculated for a PIW at 0.25 Nm and 0.5 Nm using two Sperry radar systems with short pulse setting and 24 rpm antenna rotation speed (sea state = 3).

Range (nmi)	Scans Averaged	P_{fa}/P_d PIW- March 11 Segment 1	
		VPOL 24-S	HPOL 24-S
0.25	1	0.001/ 2%	0.008 / 0%
0.25	16	0.0003/ 20%	0.0002 / 10%
0.25	32	0.0002/ 24%	0.0002 / 50%

Range (nmi)	Scans Averaged	P_{fa}/P_d PIW- March 11 Segment 1	
		VPOL 24-S	HPOL 24-S
0.5	1	0.01 / 0%	0.03 / 0%
0.5	16	0.0002/ 18%	0.0003 / 25%
0.5	32	0.0002/ 25%	0.0003 / 40%

Table XIII: P_{fa} and P_d calculated for a PIW at 0.25 Nm and 0.5 Nm using two Sperry radar systems with short pulse setting and 48 rpm antenna rotation speed (sea state = 3).

Range (nmi)	Scans Averaged	P_{fa}/P_d PIW- March 11 Segment 2	
		VPOL 48-S	HPOL 48-S
0.25	1	0.002 / 0%	0.0007 / 0%
0.25	16	0.0002 / 1%	0.0003 / 74%
0.25	32	0.0003 / 61%	0.0002 / 100%

Range (nmi)	Scans Averaged	P_{fa}/P_d PIW- March 11 Segment 2	
		VPOL 48-S	HPOL 48-S
0.5	1	0.0009 / 1%	0.0005 / 2%
0.5	16	0.001 / 1%	0.0005 / 9%
0.5	32	0.0005 / 15%	0.0002 / 84%

Table XIV: P_{fa} and P_d calculated for a PIW at 0.25 Nm and 0.5 Nm using two Sperry radar systems with medium pulse setting and 48 rpm antenna rotation speed (sea state = 3).

Range (nmi)	Scans Averaged	P_{fa}/P_d PIW- March 11 Segment 3	
		VPOL 48-M	HPOL 48-M
0.25	1	0.01 / 1%	0.001 / 0%
0.25	16	0.001 / 0%	0.0005 / 14%
0.25	32	0.003 / 0%	0.0003 / 93%

Range (nmi)	Scans Averaged	P_{fa}/P_d PIW- March 11 Segment 3	
		VPOL 48-M	HPOL 48-M
0.5	1	0.007 / 0%	0.002 / 0%
0.5	16	0.02 / 0%	0.003 / 0%
0.5	32	0.02 / 0%	0.03 / 0%

Table XV: P_{fa} and P_d calculated for a PIW at different ranges using two Sperry radar systems with short pulse setting and 24 rpm antenna rotation speed (sea state =1).

Range (nmi)	Scans Averaged	P_{fa}/P_d PIW- March 12	
		VPOL 24-S	HPOL 24-S
0.4	1	0.0001/ 78%	0.0001/ 93%
0.4	16	0.0001/ 100%	0.0002/ 100%
0.4	32	0.0001/ 100%	0.0002/ 100%
0.76	1	0.0002/ 25%	0.0002/ 62%

Range (nmi)	Scans Averaged	P_{fa}/P_d PIW- March 12	
		VPOL 24-S	HPOL 24-S
1.02	1	0.0003/ 60%	0.0002 / 50%
1.02	16	0.0001/ 100%	0.0001/ 100%
1.02	32	0.0005/ 100%	0.0001/ 100%

Table XVI: P_{fa} and P_d calculated for a PIW at 1.02 Nm using two Sperry radar systems for the data recorded on March 12 (sea state =1).

Range (nmi)	Scans Averaged	P_{fa}/P_d PIW- March 12	
		VPOL 24-M	HPOL 24-M
1.02	1	0.0003/ 33%	0.0002/ 44%
1.02	16	0.0002/ 91%	0.0003/ 100%
1.02	32	0.0002/ 100%	0.0005/ 100%

Range (nmi)	Scans Averaged	P_{fa}/P_d PIW- March 12	
		VPOL 48-S	HPOL 48-S
1.02	1	0.0003/ 34%	0.0002/ 46%
1.02	16	0.0005/ 88%	0.0001/ 100%
1.02	32	0.0003/ 100%	0.0001/ 100%

Table XVII: P_{fa} and P_d calculated for a PIW at 1.02 Nm using single Sperry radar system with vertical polarized antenna with full PRF setting (sea state =1).

Range (nmi)	Scans Averaged	P_{fa}/P_d PIW- March 12
		VPOL 24-S (Full PRF)
1.02	1	0.0002 / 38%
1.02	16	0.0004 / 88%
1.02	32	0.0001 / 97%

Range (nmi)	Scans Averaged	P_{fa}/P_d PIW- March 12
		VPOL 48-S (Full PRF)
1.02	1	0.0003 / 38%
1.02	16	0.0001 / 100%
1.02	32	0.0002 / 100%

2.2 Fast Rescue Craft (FRC)

Various pre-defined FRC routes and maneuvers (test patterns) were performed by the FRC during the Argentia trial. Most of these patterns are to be used for Target Tracker algorithm development. The set of data that is useful in this P_d analysis are from the Straight Line Tracking (SLT) pattern performed on March 9th and 12th, 2010 (see figure 9). The estimated sea states on March 9th and March 12th were 2 and 1, respectively. The SLT data included straight line radial routes traveled by the FRC and stationary positions at various ranges held by the FRC. The radial routes and stationary positions are used to calculate P_d/P_{fa} values for various ranges for this FRC target.

As with the radially moving helicopter data in Section 3.3, it is not possible to calculate a P_d value at a single range for the radial routes traveled by the FRC. Each P_d value had to be calculated over a segment of range thereby giving an average P_d value for that segment.

The results from the radial routes are shown in Table XVIII, Table XIX, and Table XX. The results from the stationary positions are shown in Table XXI. The results show that the use of scan averaging improves the P_d of the FRC target in all cases. The results obtained with the VPOL antenna have smaller P_d values than the results obtained with the HPOL antenna. It is observed that in some cases, the antenna with 24 RPM has a higher P_d value than the antenna with 48 RPM. This is because the 24 and 48 RPM data were recorded at different times and therefore had slightly different sea states which would cause the P_d to be slightly different.

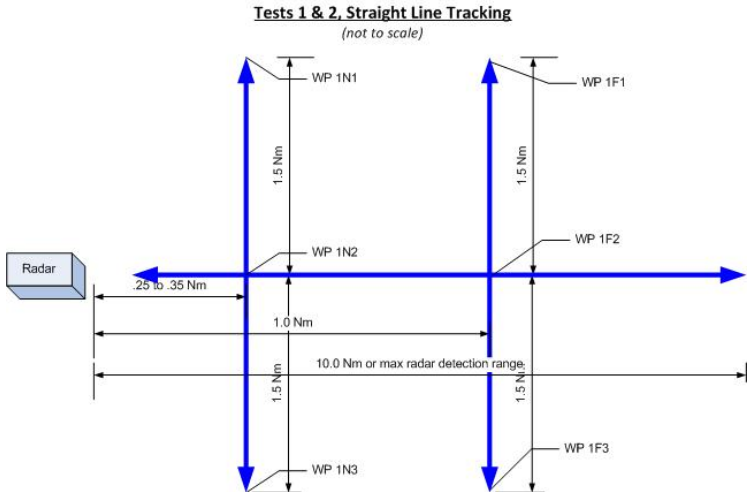

Figure 9: Straight Line Tracking (SLT) Test Pattern.

Table XVIII: P_{fa} and P_d calculated for a moving FRC at different ranges using two Sperry radar systems for the data recorded on March 12 (Sea state = 1).

Range (nmi)	P_{fa}/P_d FRC-Moving Radially SLT-RAD1-March12 Scan Averaging = 1		P_{fa}/P_d FRC-Moving Radially SLT-RAD1-March12 Scan Averaging = 4	
	VPOL	HPOL	VPOL	HPOL
	48-S	48-S	48-S	48-S
1.3-2.4	3e-5/99.7%	4e-5/99.6%	NA	NA
2.2-3.1	3e-5/98%	4e-5/99.6%	NA	NA
3.1-3.5	2e-5/92%	4e-5/99.6%	2e-5/99.8%	4e-6/100%
3.5-4.2	3e-5/66.7%	3e-5/92%	5e-5/84%	1.5e-5/99.8%
	48-L	48-L	48-L	48-L
4.2-5	0.00015/35%	0.00015/37%	0.0001/88%	0.00015/67%

Table XIX: P_{fa} and P_d calculated for a moving FRC at the speed of 22 knots at different ranges using two Sperry radar systems for the data recorded on March 12 (Sea state = 1).

Range (nmi)	P_{fa}/P_d SLT-RAD2-March12, FRC-Moving Radially VPOL 24- S (Full PRF)	
	Scan Averaging = 1	Scan Averaging = 4
1.1-2.2	4e-5/99.5%	1e-5/99.8%
2.1-3.2	1e-4/98.9%	9e-5/99%
3.2-4	7e-5/94%	1.5e-5/98%
4-4.9	1e-4/63%	1e-4/74%

Table XX: P_{fa} and P_d calculated for FRC at different ranges using two Sperry radar systems for the data recorded on March 9 (Sea state = 2).

Range (nmi)	P_{fa}/P_d FRC-Moving Radially SLT-V3_V1_out-March9 Scan Averaging = 1		P_{fa}/P_d FRC-Moving Radially SLT-V3_V1_out-March9 Scan Averaging = 4	
	VPOL	HPOL	VPOL	HPOL
	48-M	48-M	48-M	48-M
2-3.1	2.1e-5/92%	0.0001/93%	2.5e-5/100%	1e-5/100%
3.1-4	4.7e-5/67%	1.7e-5/86%	3.8e-5/99%	2.9e-6/99.2%
4-4.6	0.0001/41%	0.0001/52%	2.5e-5/54%	4.6e-5/80%
	24-S (Full PRF)	24-S		
2.7-3.8	0.00015/88.5%	0.00015/97.3%		
3.8-4.6	0.00026/49%	0.0008/73.8%		

Table XXI: P_{fa} and P_d calculated for a stationary FRC at different ranges using two Sperry radar systems for the data recorded on March 9 (Sea state = 2).

Range (nmi)	P_{fa}/P_d FRC-Moving Radially SLT-RAD1-March12 Scan Averaging = 1		P_{fa}/P_d FRC-Moving Radially SLT-RAD1-March12 Scan Averaging = 4	
	VPOL	HPOL	VPOL	HPOL
	48-M	48-M	48-M	48-M
4.2	0.00025/52%	0.0001/65%	NA	NA
4.97	0.0001/12%	0.0001/25%	0.0001/30%	0.0001/68%
	48-S (Full PRF)		48-S (Full PRF)	
4.97	7e-5/13%		7e-5/39%	

3 Skerries/Cape Spear Data Analysis

In December 2010 and January 2011, data collection trials took place off Cape Spear and at the Skerries (located just outside of St. John's Harbour). Radar data recordings of FRC, PIW, helicopter approach (HELO), and sea clutter were made. This section describes the data that was collected and the results of the analysis that was performed on the data.

During these trials, a wave buoy was placed about 0.75 Nm off of the Skerries site to record wave and current information. The Sea Clutter radar data was mostly collected at the Skerries site, and the FRC, PIW and HELO data was collected from the Cape Spear site.

One Sperry transceiver and one Consilium transceiver were used during the Skerries/Cape Spear trials. The Sperry system was capable of 24 and 48 RPM rotations rates, with two different antenna types:

- an 8ft vertically polarized antenna prototype (A1) - used for collecting PIW and FRC radar data,
- an off-the-shelf Sperry 8ft horizontally polarized antenna (H1) - used for collecting data during the HELO trial.

The Consilium system was capable of 48, 60, 80 and 120 RPM rotation rates and had an off-the-shelf Consilium 9ft horizontal polarized antenna.

3.1 Person in Water (PIW)

The PIW data recording was performed on January 26th, 2011. Figure 2 shows a picture of the PIW at the start of the trail in a sea state of 1. Two radars were used during this trial and both radars were transmitting and recording simultaneously. The Sperry system was run with the 8ft vertically-polarized antenna prototype (A1), and the Consilium system with the 9ft off-the-shelf horizontal-polarized Consilium antenna.

Figure 2: Person in the water at Cape Spear site on January 26, 2011.

Table I describes the sea states obtained by the wave buoy during this trial.

Table I: Wind Speed, and Significant Wave Height During FRC and PIW Trial

	Time (GMT)	Significant Wave height (m)	Wind Speed (knots)	Sea State
	13:30	1	0	1
	14:00	1	0.9	1
Jan 26	14:30	1	1.7	2
	15:00	1.2	1.7	2
	15:30	1.2	1.7	2

Recordings of the PIW were made at two different ranges, 1.25 Nm and 1.5 Nm. The Consilium radar recorded data at three different antenna rotation rates, 48, 60, and 120 RPM and the Sperry radar recorded data at one rotation rate, 48 RPM, as shown in Table II.

Table II: PIW trial radar settings

Run	Time (GMT)	Range	Consilium		Sperry	
			RPM	Pulse Length	RPM	Pulse Length
PIW.1	15:04	1.25 Nm	120	Short	48	Short
PIW.2	15:10	1.25 Nm	60	Short	48	Short
PIW.3	15:13	1.25 Nm	48	Short	48	Short
PIW.4	15:23	1.5 Nm	48	Short	48	Short
PIW.5	15:27	1.5 Nm	60	Short	48	Short
PIW.6	15:30	1.5 Nm	120	Short	48	Short

The calculated values of P_{fa} / P_d and the thresholds used to obtain those values are shown in Table III, Table IV, and Table V. Also, the number of scans used to calculate the P_{fa} / P_d values are shown at the last row of each table.

The results in Table III, IV, and V consistently show, at a fixed range, increasing the number of scans in the scan-to-scan integration (i.e. scan averaging) significantly improves the probability of detection of the PIW. It is observed that there is no significant difference between detection of the PIW with the VPOL antenna vs. the HPOL antenna. It is also observed that increasing the antenna rotation speed (RPM) with a fixed number of scans averaged for a stationary target (PIW) does not improve the probability of detection. It is expected that radar rotation rate should not affect probability of detection in this case since the PIW is a stationary target. It was also theorized, that if the antenna rotation speed becomes fast enough, the sea clutter will start to become correlated from scan to scan (i.e. the sea clutter doesn't change from scan to scan). If this were to occur, the probability of detection would start to decrease with higher antenna rotation rates and a fixed number of scans being averaged. It was evident from the results that in the region of 24 to 120 RPM with a low sea state of 1 to 2, the sea clutter did not become correlated and therefore the probably of detection did not start to decrease with the higher rotation rates.

Table III: P_{fa} and P_d calculated for a PIW at 1.25 and 1.5 Nm using Consilium with 120 rpm and Sperry with 48 rpm.

Range (nmi)	Scans Averaged	P_{fa}/ Threshold/ P_d PIW.1	
		VPOL 48-S	HPOL 120-S
1.25	1	3.3e-5/ 610/ 12%	2.6e-5/ 520/ 16%
1.25	16	1e-5/ 95/ 100%	1.3e-5/ 100/ 94%
1.25	32	5e-5/ 70/ 100%	2.6e-5/ 65/ 100%
1.25	64	1e-5/ 60/ 100%	3.5e-5/ 50/ 100%
Scans used		57	144

Range (nmi)	Scans Averaged	P_{fa}/ Threshold/ P_d PIW.6	
		VPOL 48-S	HPOL 120-S
1.5	1	7e-5/ 370/ 17%	7e-5/ 410/ 10%
1.5	16	1e-5/ 90/ 85%	6e-5/ 160/ 9%
1.5	32	7e-5/ 55/ 100%	8e-5/ 100/ 46%
1.5	64	1e-5/ 42 100%	7e-5/ 72/ 81%
Scans used		95	242

Table IV: P_{fa} and P_d calculated for a PIW at 1.25 and 1.5 Nm using Consilium with 60 rpm and Sperry with 48 rpm.

Range (nmi)	Scans Averaged	P_{fa}/ Threshold/ P_d PIW.2	
		VPOL 48-S	HPOL 60-S
1.25	1	3e-4/ 510/ 32%	6e-5/ 470/ 35%
1.25	16	3e-4/ 100/ 100%	3e-5/ 100/ 97%
1.25	32	6e-5/ 80/ 100%	1.5e-5/ 80/ 100%
1.25	64	4e-5/ 40 100%	3e-5/ 40/ 100%
Scans used		59	77

Range (nmi)	Scans Averaged	P_{fa}/ Threshold/ P_d PIW.5	
		VPOL 48-S	HPOL 60-S
1.5	1	1e-4/ 290/ 12%	1e-4/ 410/ 7%
1.5	16	8e-5/ 90/ 30%	6e-5/ 120 36%
1.5	32	6e-5/ 60 71%	7e-5/ 100/ 44%
1.5	64	3e-5/ 50/ 36%	7e-5/ 65/ 55%
Scans used		80	103

Table V: P_{fa} and P_d calculated for a PIW at 1.25 and 1.5 Nm using Consilium and Sperry both with 48 rpm.

Range (nmi)	Scans Averaged	P_{fa}/ Threshold/ P_d PIW.3 VPOL 48-S	P_{fa}/ Threshold/ P_d PIW.3 HPOL 48-S
1.25	1	3e-5/ 450/ 11%	8.6e-5/ 540/ 14%
1.25	16	2e-5/ 110/ 58%	2e-5/ 130 58%
1.25	32	3e-5/ 80/ 70%	2e-5/ 100/ 67%
1.25	64	8e-5/ 60/ 83%	9e-6/ 70/ 82%
Scans used		130	130

Range (nmi)	Scans Averaged	P_{fa}/ Threshold/ P_d PIW.4 VPOL 48-S	P_{fa}/ Threshold/ P_d PIW.4 HPOL 48-S
1.5	1	2e-5/ 370 14%	3e-5/ 450/ 16%
1.5	16	4e-5/ 80/ 79%	6e-5/ 100/ 98%
1.5	32	2e-5/ 60 93%	1e-5/ 80/ 100%
1.5	64	1e-5/ 50/ 93%	5e-6/ 70/ 100%
Scans used		97	97

3.2 Fast Rescue Craft (FRC)

The FRC data recording was performed on January 26th, 2011. Table I displays the sea states obtained during the trial by the wave buoy at the Skerries site. The FRC route test pattern is shown in Fig. 3. The FRC route was run multiple times with four different antenna rotation speeds, i.e. 48, 60, 80 and 120 rpm as shown in Table VI.

Table VI: FRC Trial

Run	Time (GMT)	Direction	Range	Consilium RPM	Consilium Pulse Length	Sperry RPM	Sperry Pulse Length
FRC.1	13:24 - 14:18	Out	0 to 5 Nm	80	Short	48	Short
FRC.2	14:20 – 14:50	In	5 to 0 Nm	120	Short	48	Short
FRC.3*	15:43 – 16:14	Out	1 to 5 Nm	60	Short	48	Short

***Note: FRC was carrying the radar reflector buoy when executing FRC.3**

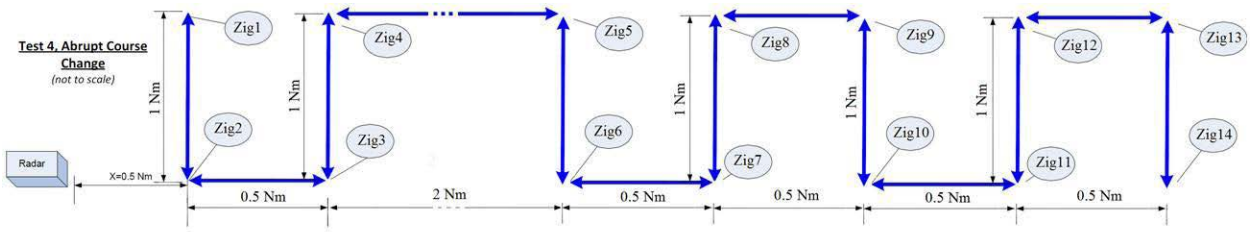

Figure 3: FRC course during the trial on January 26.

In order to calculate meaningful P_d and P_{fa} values for a moving target, the target must be analyzed over a section of its travel that is of constant range from the radar since P_d is a function of target range. To do this, the P_d and P_{fa} are calculated for the target traveling along the transverse segments only. In order for Scan averaging to be most effective (when used on a moving target), the target must occupy only one radar resolution cell during the period of the scan averaging. If the target moves through more than one resolution cell the return signal gets blurred and the signal to noise ratio decreases. For a target with a constant speed, the maximum number of scans that can be averaged (the number of scans that target remain in one resolution cell) depends on the antenna rotation speed. The higher the antenna rotation speed is, the greater the number of scans that can be averaged. For example, for a target moving azimuthally with the maximum speed of 25 knots, the maximum number of scans that can be integrated are 4, 5, 7, and 11 for the antenna rotation speeds of 48, 60, 80, and 120 rpm, respectively.

The P_d and P_{fa} results for this trial are shown in Table VII, Table VIII, and Table IX. In all cases, we see that scan averaging improves the radar performance significantly. With this target and sea state we see an increase in detectable range of about 1.5 to 2.0 Nm when scan averaging is applied.

Table VII: P_{fa} and P_d calculated for a moving FRC at different ranges using Consilium and Sperry radar systems with short pulse and antenna rotation speed of 80 rpm and 48 rpm, respectively. The HPOL data was missing scans and the corrupted images were not included in the processing.

Range (Nm)	P_{fa}/P_d FRC.1					
	Scan Averaged = 1		Scan Averaged = 4	Scan Averaged =7	Number of Scans Used	
	VPOL 48-S	HPOL 80-S	VPOL 48-S	HPOL 80-S	VPOL 48-S	HPOL 80-S
1.0	1e-5/ 100%	3e-5/ 100%	4e-5/ 100%	5e-5/ 100%	58	78
3.0	2e-5/ 99%	3e-5/ 94%	1e-5/ 100%	1e-5/ 100%	93	117
3.5	2e-5/ 95%	2e-5/ 97%	2e-5/ 100%	2e-5/ 100%	97	116
4.0	2e-5/ 89%	2e-5/ 88%	1.5e-5/ 100%	Data Corrupted	95	NA
4.5	2e-5/ 79%	2e-5/ 84%	1.5e-5/ 100%	1.6e-5/ 100%	95	101
5.0	1.3e-5/ 65%	1.3e-5/ 60%	2e-5/ 90%	2e-5/ 100%	108	147
5.5	1.7e-5/ 38%	1.5e-5/ 55%	4e-5/ 77%	2e-5/ 93%	124	190

Table VIII: P_{fa} and P_d calculated for a moving FRC at different ranges using Consilium and Sperry radar systems with short pulse and antenna rotation speed of 120 rpm and 48 rpm, respectively.

Range (Nm)	P_{fa}/P_d FRC.2					
	Scan Averaged = 1		Scan Averaged = 4	Scan Averaged =11	Number of Scans Used	
	VPOL 48-S	HPOL 120-S	VPOL 48-S	HPOL 120-S	VPOL 48-S	HPOL 80-S
1.0	6e-5/ 100%	4e-5/ 100%	6e-5/ 100%	4e-5/ 100%	79	200
3.0	2e-5/ 100%	3e-5/ 100%	4e-5/ 100%	2e-6/ 100%	108	276
3.5	1e-5/ 96%	3e-5/ 93%	3e-5/ 100%	5e-5/ 100%	112	282
4.0	3e-5/ 88%	3e-5/ 91%	1e-5/ 99%	6e-6/ 100%	107	269
4.5	1.5e-5/ 77%	1.8e-5/ 72%	5e-5/ 100%	1.8e-5/ 98%	99	247
5.0	1.5e-5/ 56%	1e-5/ 54%	1.5e-5/ 90%	3e-5/ 93%	87	221
5.5	2.2e-5/ 35%	2e-5/ 44%	4.5e-5/ 76%	1.6e-5/ 91%	134	339

Table IX: P_{fa} and P_d calculated for a moving FRC carrying a reflector buoy using Consilium and Sperry radar systems with short pulse and antenna rotation speed of 60 rpm and 48 rpm, respectively.

Range (Nm)	P_{fa}/P_d FRC.2					
	Scan Averaged = 1		Scan Averaged = 4	Scan Averaged =5	Number of Scans Used	
	VPOL 48-S	HPOL 60-S	VPOL 48-S	HPOL 60-S	VPOL 48-S	HPOL 80-S
1.0	3e-5/ 100%	4e-5/ 100%	3e-5/ 100%	2e-5/ 100%	103	133
3.0	2e-5/ 99%	5e-5/ 100%	3e-5/ 100%	5e-6/ 100%	82	165
3.5	2e-5/ 98%	2e-5/ 98%	2e-5/ 100%	2e-5/ 100%	112	145
4.0	2e-5/ 88%	2e-5/ 94%	4e-6/ 100%	4e-6/ 100%	107	138
4.5	3e-5/ 77%	3e-5/ 84%	3e-5/ 100%	3e-5/ 100%	131	169
5.0	1.5e-5/ 73%	1.5e-5/ 74%	4e-5/ 98%	6e-6/ 100%	79	104
5.5	3e-5/ 47%	2e-5/ 66%	4e-5/ 83%	3e-5/ 100%	117	151

Fig. 4 shows the comparison between the P_d values obtained for vertical and horizontal polarizations. It is observed that the vertically and horizontally polarized radars have approximately the same P_d value out to 5 Nm. At the 5.5 Nm range (the maximum range tested) the horizontal polarized radar system has slightly larger P_d value compared to the vertically polarized radar system. This increase of P_d value seems to extend back to 5 Nm when scan averaging is applied. The difference in P_d at larger ranges is due to the fact that the sea clutter in the VPOL images extends to a further distance than the HPOL images.

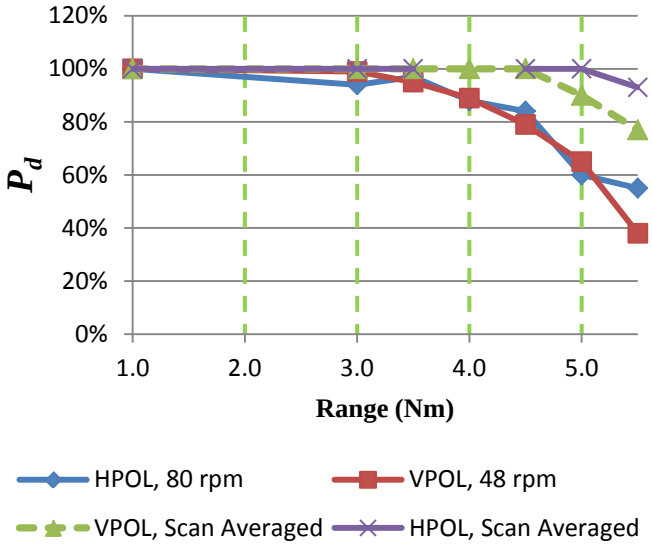

(a)

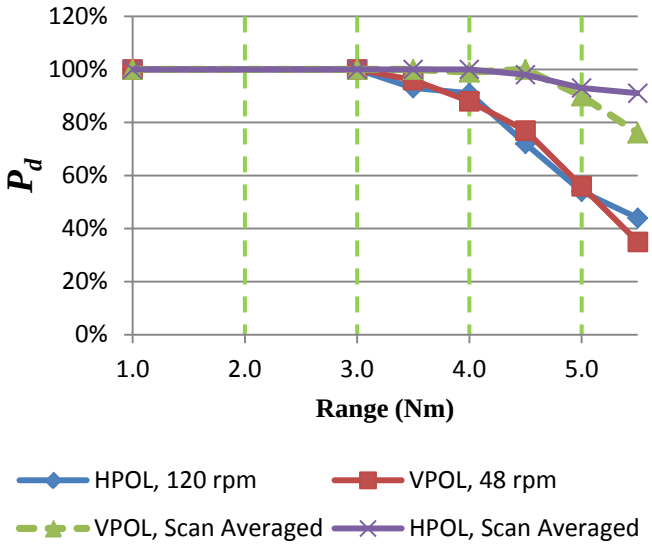

(b)

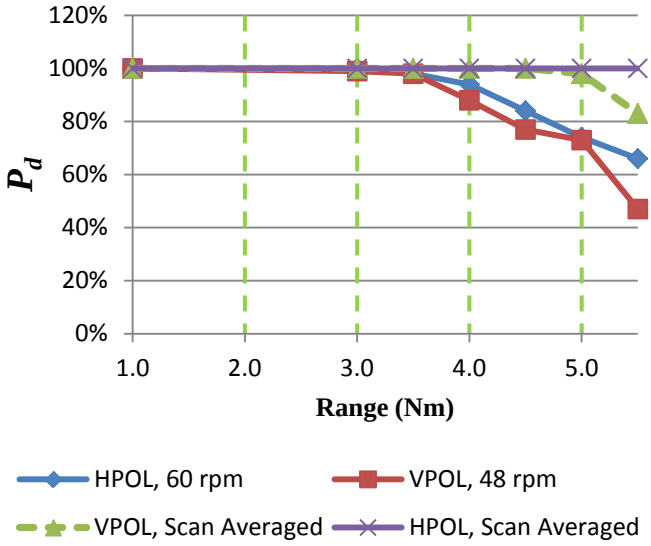

(c)

Figure 4: P_d versus range comparing vertical and horizontal polarizations for (a) FRC.1, (b) FRC.2, and (c) FRC.3. The Scan averaging improves the performance for all cases.

Fig. 5 compares the P_d values for the three separate FRC runs of the same scenario where the Consilium radar was run at three different rotation rates. The Consilium radar results (as shown in Fig. 5b) show that the P_d values for the three runs are similar up to 4 Nm. Past 4 Nm we see that the 3rd run (at 60RPM) has slightly higher P_d values. However we see the same trend with the Sperry radar (with vertical polarized antenna) which was run at the same 45 RPM for all three runs (as shown in Fig. 5a). This shows that the differences in P_d were due to differences in sea state and other factors and not due to differences in antenna rotation speed. It can therefore be concluded that in this case the antenna rotation speed does not improve the radar performance.

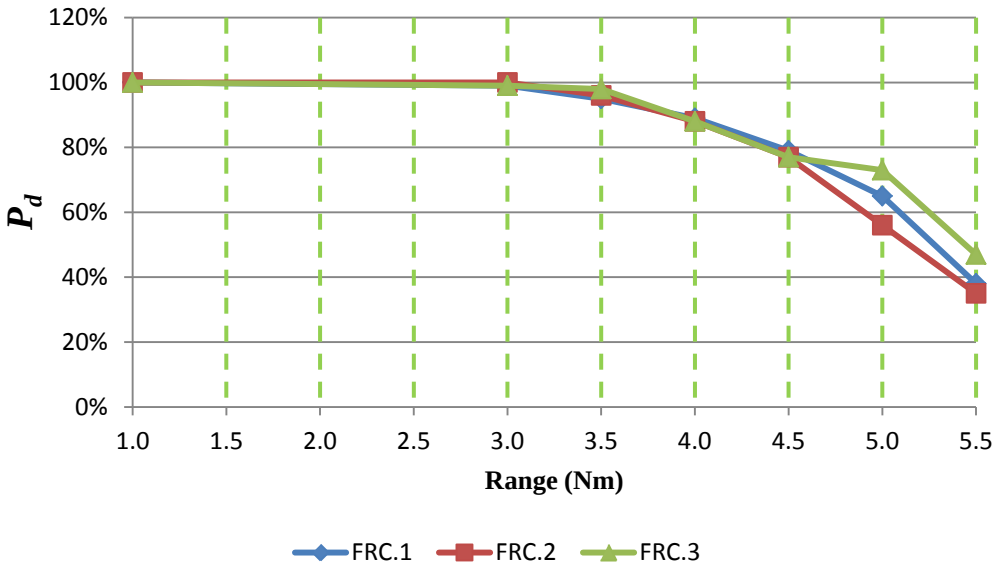

(a)

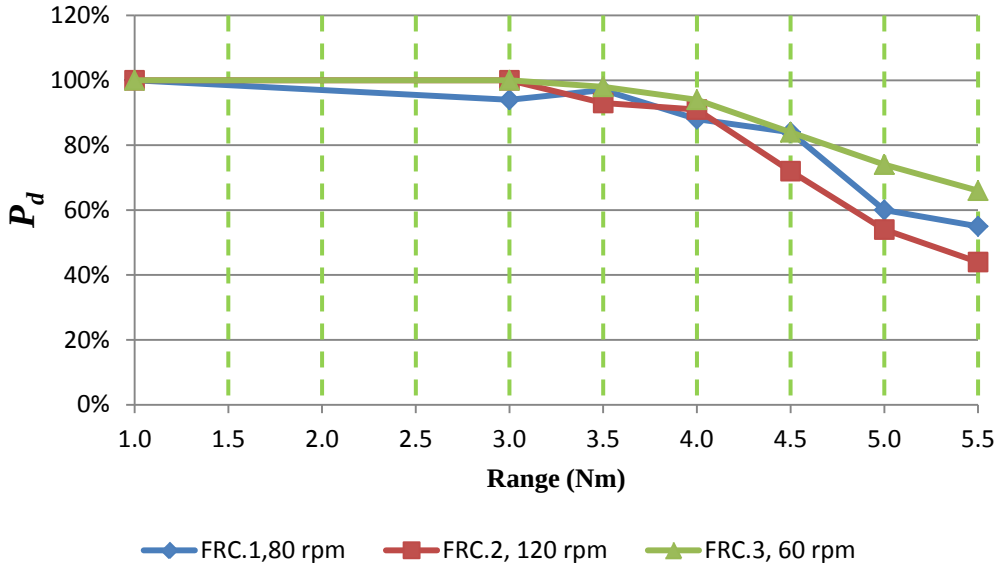

(b)

Figure 5: P_d versus range comparing three scenarios for (a) Sperry, and (b) Consilium radar systems. No scan averaging has been used.

3.3 Helicopter Trial (HELO)

The helicopter data recording was performed on January 25th, 2011. The purpose of this trial was to test the detectability of a helicopter using a commercial marine navigation radar. The helicopter executed three straight line runs that followed a flight path that mimicked a helicopter landing approach to an offshore vessel (as shown in Fig. 6). The wave buoy at the Skerries site measured a sea state of 4 during this trial. During each run the helicopter was moving radially away from the radar at a fixed azimuth and a fixed speed of 90 knots. Since the helicopter was moving radially away from the radar it is not possible to calculate a P_d value at a single range. Each P_d value had to be calculated over a segment of range thereby giving an average P_d value for that segment.

The P_d and P_{fa} results are shown in Table X and Figure 7. The results show that the P_d for the Helicopter was fairly low out to approximately 5 Nm. This was due to the high amount of sea clutter (measured sea state = 4). Between 5 and 10 Nm the P_d was between 90 and 100%. Then Past 10 Nm the P_d starts to diminish due to weaker radar returns.

The helicopter data was also analyzed in a qualitative way. The radar data was played back and observed on the Rutter radar display to determine how easily a trained radar operator could identify the helicopter target from the surroundings and follow it throughout the flight path. From 0 – 4 Nm the HELO target is of similar size and intensity as the most intense sea clutter (sea state 4). At these ranges the HELO blends into the clutter fairly well but an experienced radar operator would be able to detect and follow the HELO fairly easily. From 4 - 6.5 Nm the HELO is out of the clutter region and is easily identified and followed. From 6.5 – 9 Nm the target intensity starts to oscillate from full intensity to almost zero at Short pulse length. An experienced operator can easily follow the HELO at these ranges but the HELO almost disappears at certain times. After 9 Nm in Short pulse length the target is visible less than 50% of the time. In medium pulse the target oscillation range is increased to about 9 – 12 Nm. After 12 Nm the target is visible less than 50% of the time in Medium pulse. In Long pulse the target oscillation range increases to about 11 – 14 Nm. After 14Nm the target is visible less than 50% of the time in Long pulse length. Then past 17 Nm the target is no longer visible. Table XI shows a summary of these qualitative observations.

The minimum observable range of the helicopter target was approximately 0.08 Nm with the target elevation of 120 ft. This gives a maximum detectable elevation angle of 13.9° as shown in Fig. 6. This is in agreement with the Vertical Beam width of the Consilium radar antenna which has a -3dB elevation angle of 11°.

The use of scan averaging to enhance the detectability in the clutter zone was found not to be useful due to the high speed of the target. Even with minimal scans averaged the target would blur, reducing the target intensity and therefore the signal to clutter level.

Table X: Calculated P_{fa} /P_d for HELO-1 trial using Consilium radar

Range (Nm)	Altitude (ft)	HELO-1, Jan 25 HPOL 60 rpm	
		P_{fa}/P_d	Number of Scans
0.3-0.76 Short	<400	6.5e-5/ 40%	26
0.68-1.36 Short	<500	6.3e-5/ 88%	44
1.36-2.5 Short	<1000	3.6e-5/ 59%	59
2.5-4.4 Short	500 to 1000	3.7e-5/ 48%	75
5.5-6.7 Short	1000 to 1500	1.1e-5/ 94%	53
7.1-8.1 Short	1500 to 2000	2.2e-5/ 100%	49
10.2-13.9 Medium	2200	1.6e-5/ 73%	131
12.9-15.5 Long	2200	7e-5/ 35%	105

Table XI: Observation on radar performance for HELO trial

Range	0 - 0.08	0.08- 4	4-6.5	6.5-9	9-12	11-14	14-17	>17
Pulse Length	Short	Short	Short	Short	Medium	Long	Long	Long
Target blob	Not Visible	Solid, Similar to Clutter	Solid	Oscillating Intensity	Oscillating Intensity	Oscillating Intensity	< 50% Visible	Not Visible
Operator Detection	None	Visible Difficult	Visible Easy	Visible Some Difficulty	Visible Some Difficulty	Visible Some Difficulty	Hard	None

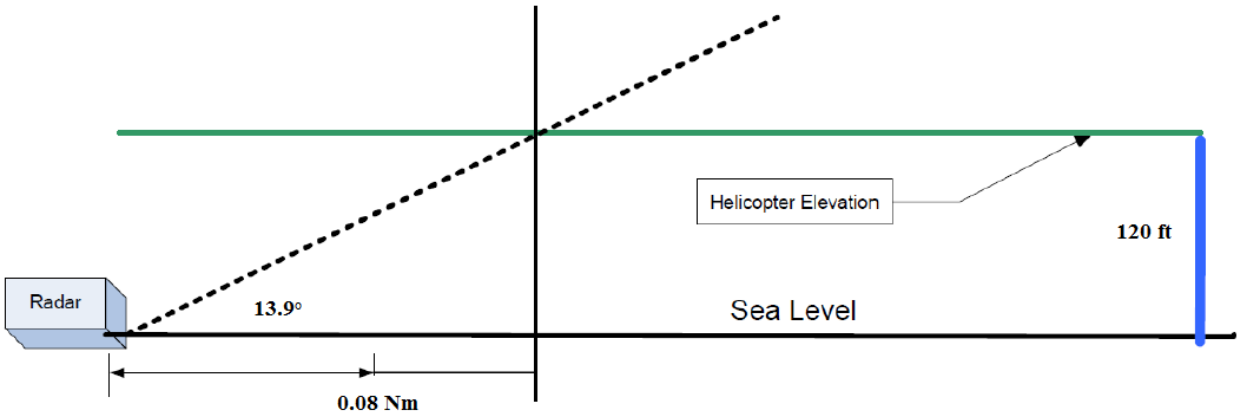

Figure 6: HELO course for defining the maximum detectable elevation angle during the trial.

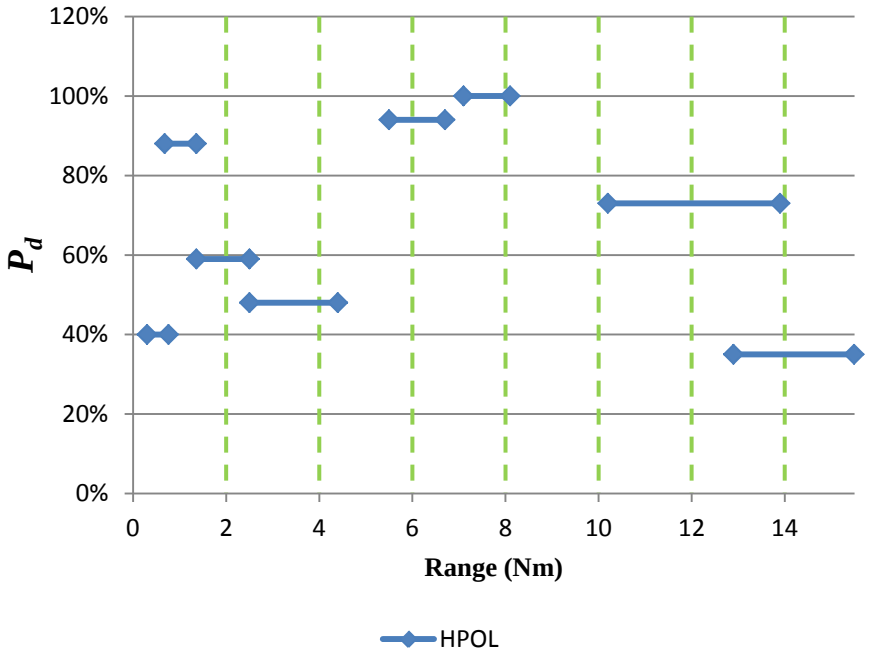

Figure 7: P_d versus range for HELO trial using Consilium radar system. No scan averaging has been used.

4 Conclusions

The analysis results obtained for the data collected at Cape Spear show that the two radar systems (Consilium transceiver with a horizontal polarized antenna and a Sperry transceiver with the A1 vertical polarized antenna) have very close performance in detecting the PIW and FRC targets in low sea states (these were the only sea states that occurred during the testing). The results suggest that the vertical polarized antenna is just as effective for target detection as a horizontally polarized antenna in these low sea states (1 and 2) and at close ranges. However, in the FRC data we see the P_d value of the HPOL diverge from and become greater than the VPOL value at the furthest range. The difference in P_d at the furthest range is due to the sea clutter in the VPOL images extending to a further distance than in the HPOL images.

The data recorded at Argentia was contaminated by the side lobe of the P13 vertical polarized antenna. This degraded the probability of detection obtained for the PIW and FRC with the vertical polarized antenna. These results should therefore not be used to compare target detection of VPOL vs. HPOL.

In all cases, the scan-to-scan processing (i.e. scan averaging) significantly improved the probability of detection.

It is observed that increasing the antenna rotation speed (RPM) with a fixed number of processed scans for a stationary target (PIW) does not improve the probability of detection. It was theorized that if the antenna rotation speed is becomes fast enough the sea clutter will start to become correlated from scan to scan (i.e. the sea clutter doesn't change from scan to scan). It was evident from the results, that in the region of 24 to 120 RPM with a low sea state of 1 to 2, the sea clutter did not become correlated and therefore did not affect the probably of detection.

For the FRC (fast target), it was theorized that a faster antenna rotation speed would allow a greater number of scans to be integrated, for the same amount of target movement, and therefore an improvement in detectability should be observed. However, the results show that the improvement is not significant. Since the trial data only included a few low sea states, the effect of the radar RPM on target P_d could not be fully studied. There is still the possibility that the radar RPM may have more of an effect on target detection with higher sea states.

The results of the Helicopter trial showed that commercial marine navigation radar may be useful for tracking a helicopter during an offshore vessel landing approach. The helicopter became detectable in the 10 to 12 Nm range and was easily detected and followed from 10 to 5 Nm. Once the helicopter entered the sea clutter region of the radar (0 to 5 Nm) the detectability decreased to between 50 and 90% for a moderate sea state of 4. This is at the limit of detectability but the detectability would increase for lower sea states. The use of Scan averaging to enhance the detectability in the clutter zone was found not to be useful due to the high speed of the target.

5 Future Work

In future, it would be useful to record more FRC data at higher sea states to further study the effect of RPM on P_d for a moving target.

All the data collected and recorded for wave spectra analysis contains scans with a fixed high-flyer buoy and the wave buoy. These targets can be used to further study the effect of antenna rotation speed on radar performance for a stationary target with different sea states.

If needed, the RCS of the PIW and FRC targets could be calculated from the recorded data. The measured reflected power can be extracted from the recorded radar data using the calibration curves. The RCS can then be obtained by modeling the reflected signal power from the target using the Carpet software.

Comparing the recorded images from VPOL and HPOL radar systems, it is observed that the VPOL radar is able to image the actual sea waves and swells very well. However, the sea clutter from the HPOL radar is much noisier and the image of the wave and swell pattern is not apparent. In the future, it might be possible to develop an algorithm to significantly suppress the sea clutter from a VPOL radar since the behavior of the wave pattern and therefore the sea clutter can be predicted using Wave Spectra software.

In future, it will be useful to compare the experiment results (the P_d results) obtained for different amounts of scan averaging to the theory and the S6 computer model that we use to simulate the effect of scan averaging on P_d values.

It was observed that the sea bird blobs were bigger on the HPOL images than the sea bird blobs on the VPOL scans. In future, it could be useful to compare the VPOL and HPOL results containing sea birds. This might provide evidence that it is better to use VPOL antennas in applications where birds interfere with target detection.

Appendix A: Radar Calibration Curves

A1. Introduction

Rutter Inc. ("Rutter") spent the months of December and January in the field collecting radar target data of fast rescue craft (FRC), person in water (PIW), helicopter approach (HELO), and wave spectra data recordings. All recordings were performed using two radar systems, namely Sperry and Consilium. In order to compare the results obtained from the two radars, calibration procedure was performed on March 10, 2011. The purpose of the calibrations was to measure and compare the performances of the two radar receivers.

This report documents the curves showing the receiver performance of the two radars and is intended to provide supporting information for future users of the dataset.

A2. Test Sites and Scenarios

Calibration took place on a runway at Bell Island. The tests were conducted using three scenarios.

The first scenario used an Agilent E8257D signal generator placed on the runway 400 m away from the radar van. Fig. 1 shows the test site and the location of the radar van and signal generator. Signal generator was connected to a horn antenna transmitting a horizontal polarization as shown in Fig. 1.b. The signal generator was transmitting a pulse with period of 40 μs and pulse width of 1 μs. The signal generator ALC (automatic level control) was on. ALC provides the signal generator with an accuracy of +/-0.15 dB (typical) output power. The Consilium and Sperry radar systems with horizontal antennas were operating at 9.373 and 9.41 GHz, respectively. While each radar system was recording data, the other radar was turned off. The two radars were sector blanked from 0 to 360° (They were not transmitting). The INI files used for calibration were the same as used in Sea Trial, on January 26, 2011.
This first scenario was later repeated close to Kelsey Drive (on April 7th and 8th), St. John's, when the pulse width was set to 50 ns.

a) **b)**

Figure 1: First scenario. a) Location of the truck and signal generator at Bell Island with a 400 meter clear range from the radar van to signal generator. b) Signal generator connected to a horn antenna in front of a truck, transmitting a reference signal 400 m away from the radar van.

The second scenario was conducted with both radars working simultaneously with no sector blanking (both radars were transmitting). The signal generator and the horn antenna were replaced with a Luneberg lens that was placed at ranges (R= 300 m, 400 m, and 500 m) away from the radar van (At 400 m, the lens was placed at the exact location and height of the horn). Fig. 2 shows the radar van and the Luneberg lens on the runway.

The third scenario was conducted inside the truck. The signal generator was used to inject a pulse into the Consilium radar transceiver only (the Sperry transceiver hardware did not have a means of injecting a signal at this point in the hardware), as shown in Figure 3. The radar was sector blanked from 0 to 360° (it was not transmitting) and the radar data were recorded. Pulse widths of 50 ns, 250 ns, and 750 ns were used when the radar was on Short, Medium, and Long pulse mode, respectively. The frequency of the signal generator was set to 9.373 GHz. The signal generator Power Search function was set to "automatic" with ALC off. Power Search is a calibration routine that improves level accuracy with ALC off and provides the signal generator with a power output accuracy of +/-0.5 dB (typical). The signal generator pulse was triggered by the internal trigger pulse of the Consilium transceiver with a delay of 62 μs so that the injected pulses generated a ring at 5 Nm on the radar screen as shown in Fig. 4.

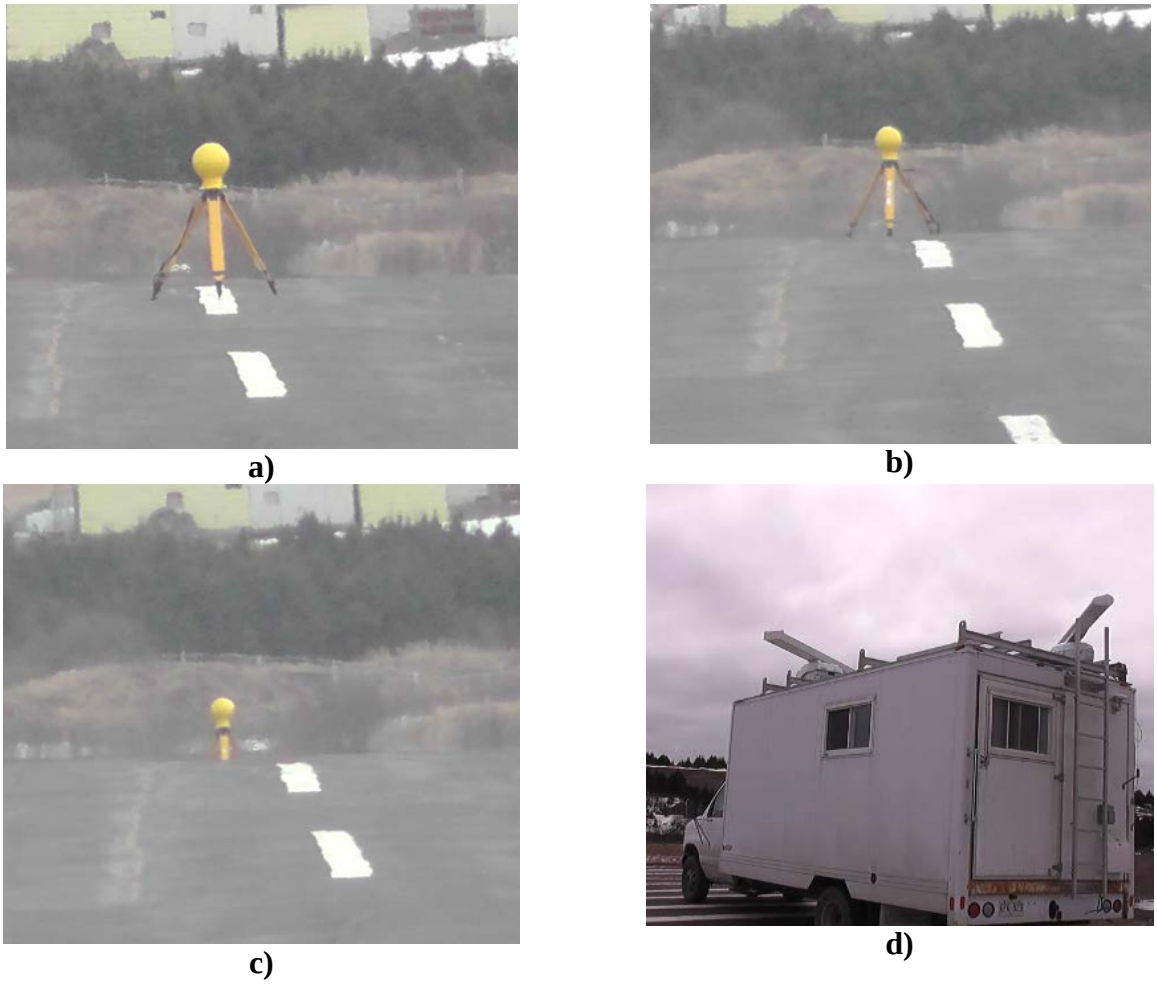

Figure 2: Second scenario. Location of the Luneburg Lens on the runway at a) 300 m, b) 400 m, c) 500 m, away from the radar van. d) Radar van with two radar systems, both transmitting horizontal polarization.

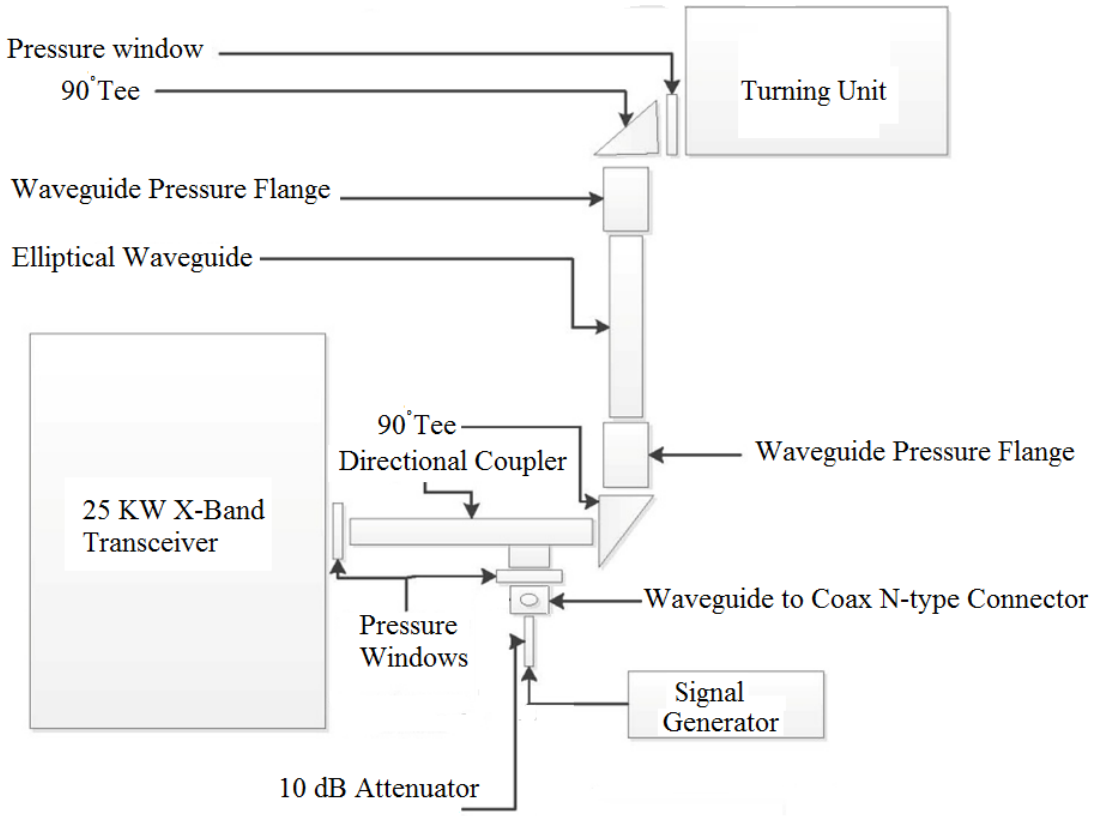

Figure 3: Set up for the third scenario. Pulse injected by the signal generator is recorded by Consilium radar.

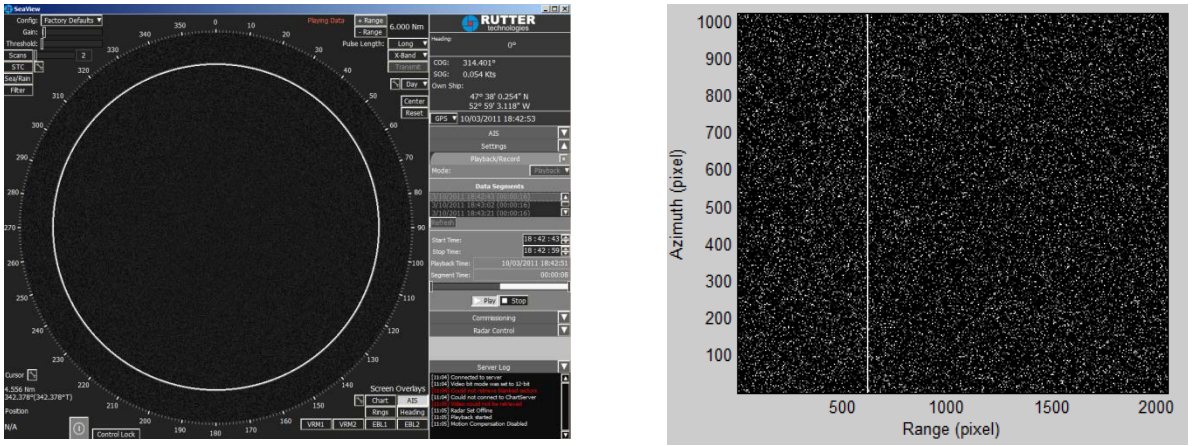

a) **b)**

Figure 4: Radar data recorded during the third scenario. a) Scan converted image, b) B-scan image.

A3. Results

The calibration results and curves were obtained using MATLAB software and the Sigma S6 Server software with all processing turned off.

A3.1 First Scenario

This test was performed to obtain the slope of the receiver calibration curve for the Sperry radar. We refer to this slope as the "magic number". The magic number is the number of radar image grey scale intensity levels which correspond to a rise of 1 dB of power at the receiver. To have a better amplitude level accuracy of the transmitted signal, the signal generator ALC was on. But the ALC function could only be used with a pulse that had a width of 1 μs or larger. Therefore a pulse with of 1 μs was chosen for the transmitted pulse.

There was concern that calibrating the radar using a generated pulse that had a longer pulse width than the radar pulse width would affect the results. We therefore did a comparison to check if this would affect the magic number calculation. Fig. 5 shows the comparison of the calibration curves when the signal generator (SG) was transmitting a signal with the pulse widths of pw = 50 ns and 1 μs, and the radar on short pulse. The dashed line corresponds to the recorded data on April 7th, while the solid blue curve shows the results obtained from April 8th recordings. Moreover, Fig. 6 shows the same comparison between the calibration curves when the transmitting pulse had a pulse width of pw = 250 ns and 1 μs, and radar setting was on medium pulse. Each data point was obtained by taking the maximum intensity level of the azimuth data along the main beam direction, and taking median value over 30 scans. The results show that the slopes of the obtained calibration curves are very similar. Note that the curves have been horizontally shifted since the distance from the SG to the radar van was different in each trial. This was not an issue since the objective of this test was to obtain the slope of the curves only and not the absolute values. This suggests that the data obtained using a pulse width of 1 μs is valid and is not changed due to the pulse width being different than the pulse width normally output by the radar transceiver.

Fig. 7 shows the long-pulse calibration-curve for the Sperry radar obtained from the data recorded at Bell Island on March 10, 2011. The transmitted pulse had a pulse width of pw = 1 μs. Fig. 8 shows the short-pulse calibration-curve for Consilium radar obtained from the data recorded at Bell Island on March 10, 2011. The transmitted pulse had a pulse width of pw = 1 μs. Fig. 9 compares the curves obtained for Sperry radar when the radar setting was on short, medium, and long pulse lengths.

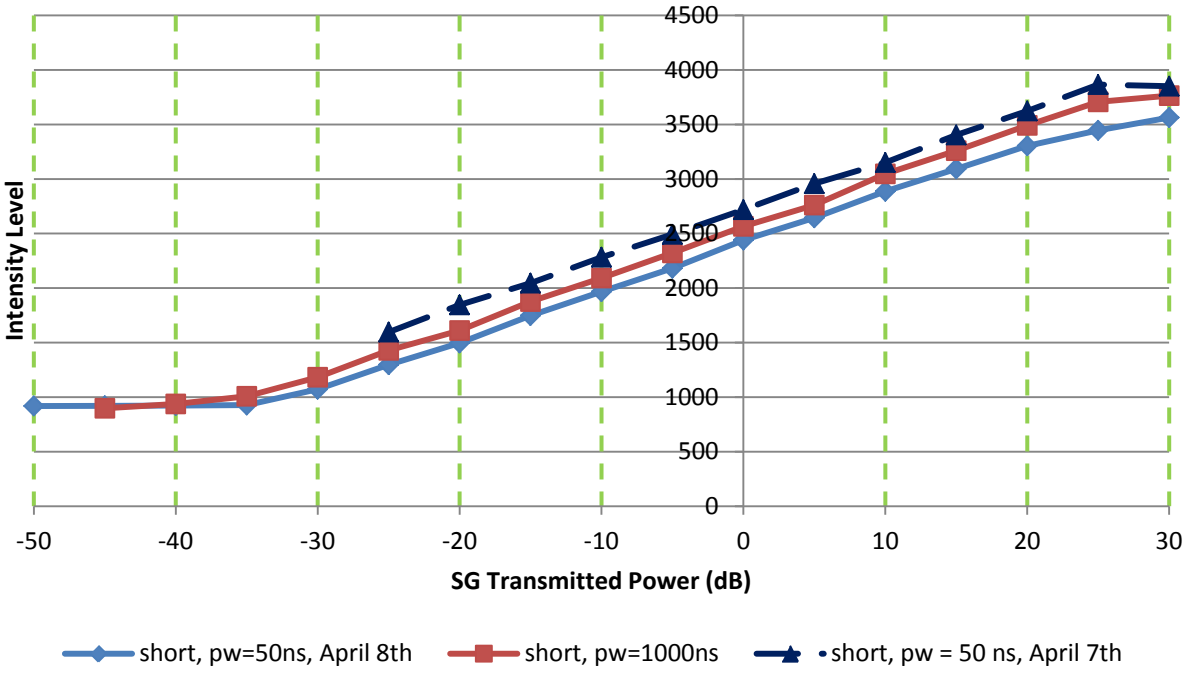

Figure 5: Sperry radar calibration data recorded when the signal generator was transmitting a signal with a pulse width of *pw* = 50 ns (at Kelsey Drive), and *pw* = 1µs (at Bell Island).

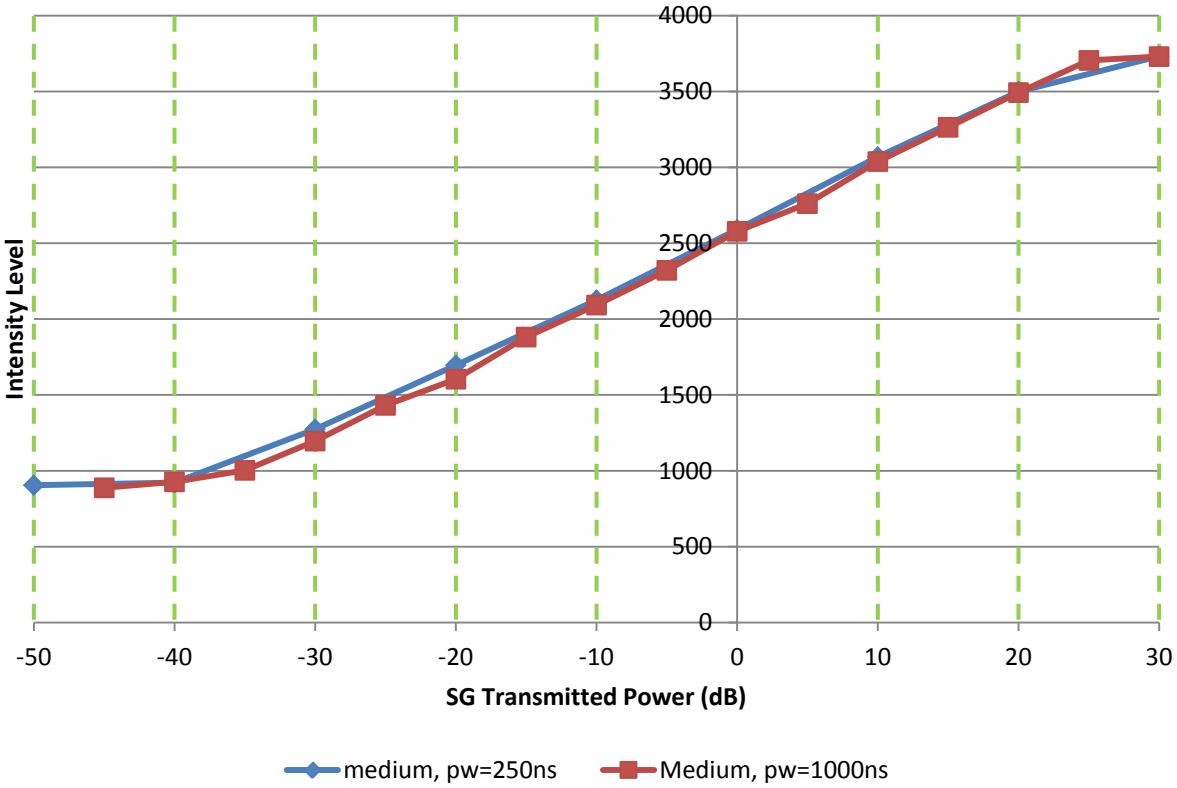

Figure 6: Sperry radar calibration data, recorded when the signal generator was transmitting a signal with a pulse width of *pw* = 250 ns (at Kelsey Drive), and *pw* = 1µs (at Bell Island).

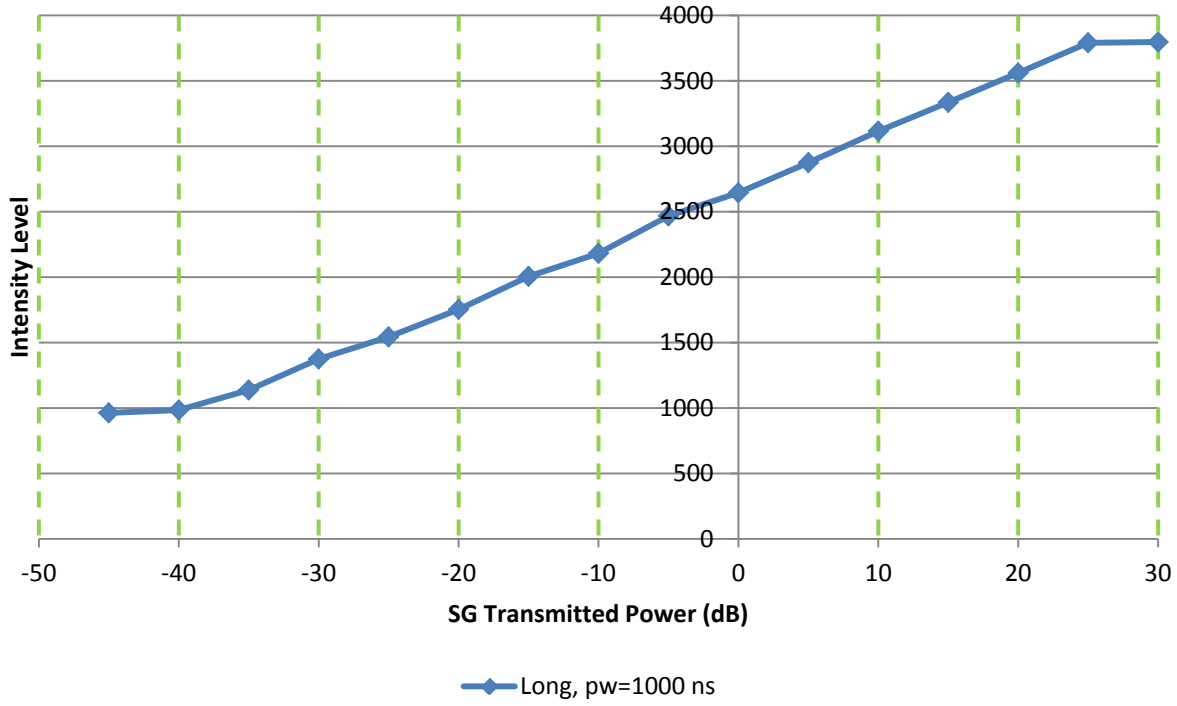

Figure 7: Sperry radar calibration data, recorded when the signal generator was transmitting a signal with a pulse width of *pw* = 1μs (at Bell Island), and the radar was on long pulse.

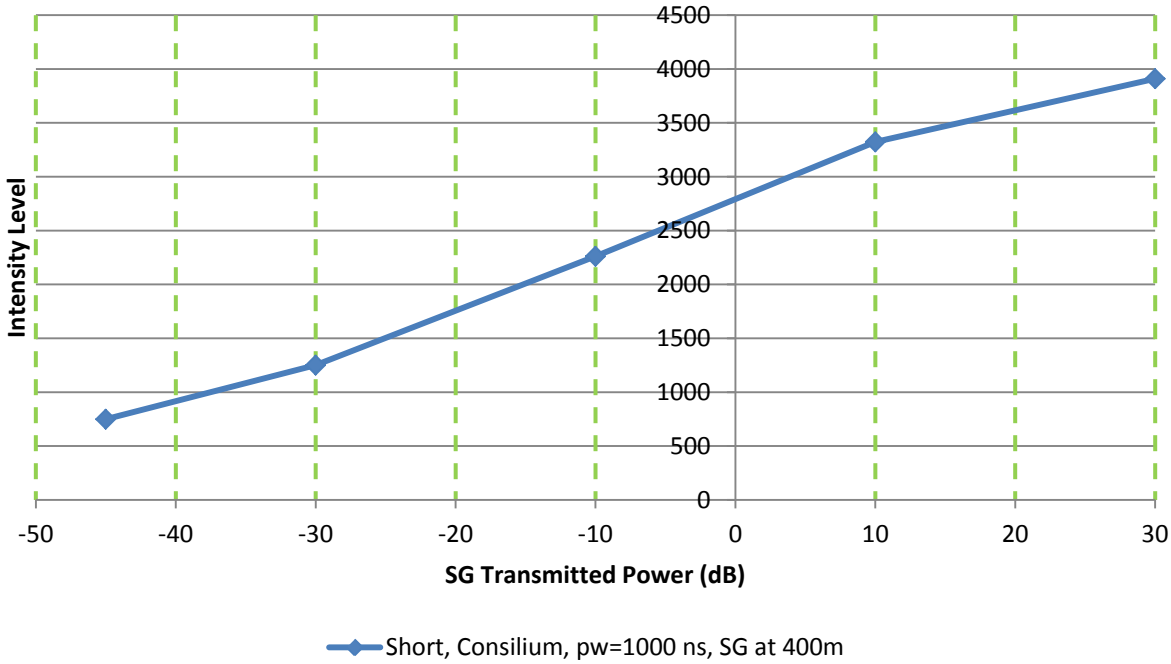

Figure 8: Consilium radar calibration curve, recorded when the signal generator was at a distance *d* =400 m, transmitting a signal with a pulse width of *pw* = 1 μs (at Bell Island), and the radar was on short pulse.

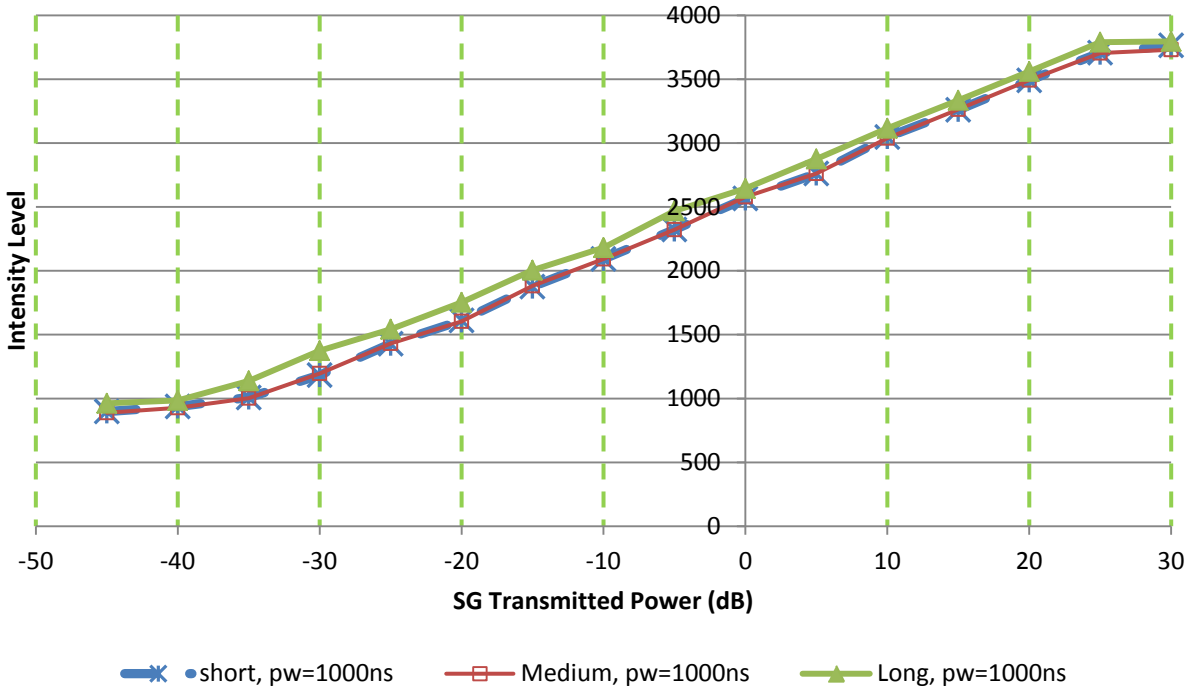

Figure 9: Comparing Sperry radar calibration curves, recorded when the signal generator was at a distance *d* =400 m, transmitting a signal with a pulse width of *pw* = 1 µs (at Bell Island), and the radar was on short, medium and long pulse.

A3.2 Second Scenario

The second scenario was conducted at Bell Island with the two radars transmitting simultaneously, when the Luneberg lens was placed at R = 300 m, 400 m, and 500 m. Table I shows the median of the maximum intensity levels measured over 90 scans.

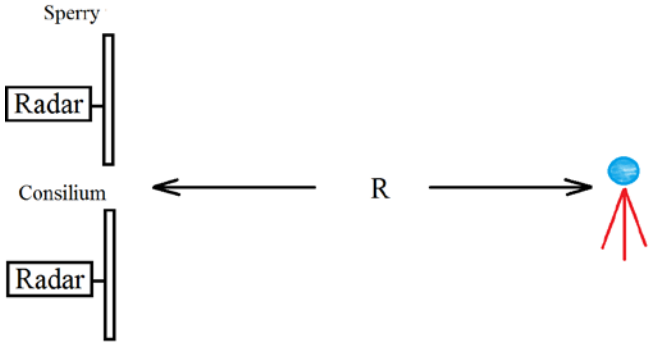

Figure 10: The two radars transmitting simultaneously in front of the Luneberg lens at a distance R.

Table I: Median of the Maximum Intensity Levels Obtained Over 90 Scans

		300 m	400 m	500 m
Sperry	**Short**	2551	3899	3095
	Medium	2607	4095	3344
	Long	2812	4095	3474
Consilium	**Short**	3163	3978	3472.5
	Medium	3705	4095	4061
	Long	3547.5	4095	3887

Table II: Variance of the Maximum Intensity Levels Obtained Over 90 scans

		300 m	400 m	500 m
Sperry	**Short**	38	45	61
	Medium	31	NA	39
	Long	37	NA	18
Consilium	**Short**	13	9	13
	Medium	15	NA	20
	Long	58	NA	58

Note: the NA values in Table II are due to the recorded intensity level being at Saturation (4096)

A3.3 Third Scenario

The amplitude calibration was performed on the Consilium radar by using the signal generator to inject pulses into the radar through the directional coupler as shown in Fig 3. The injected signal had a pulse width of 60 ns, 250 ns, and 750 ns when the radar was on short, medium, and long pulse, respectively. The curves obtained for the short, medium, and long pulse are shown in Fig. 11.

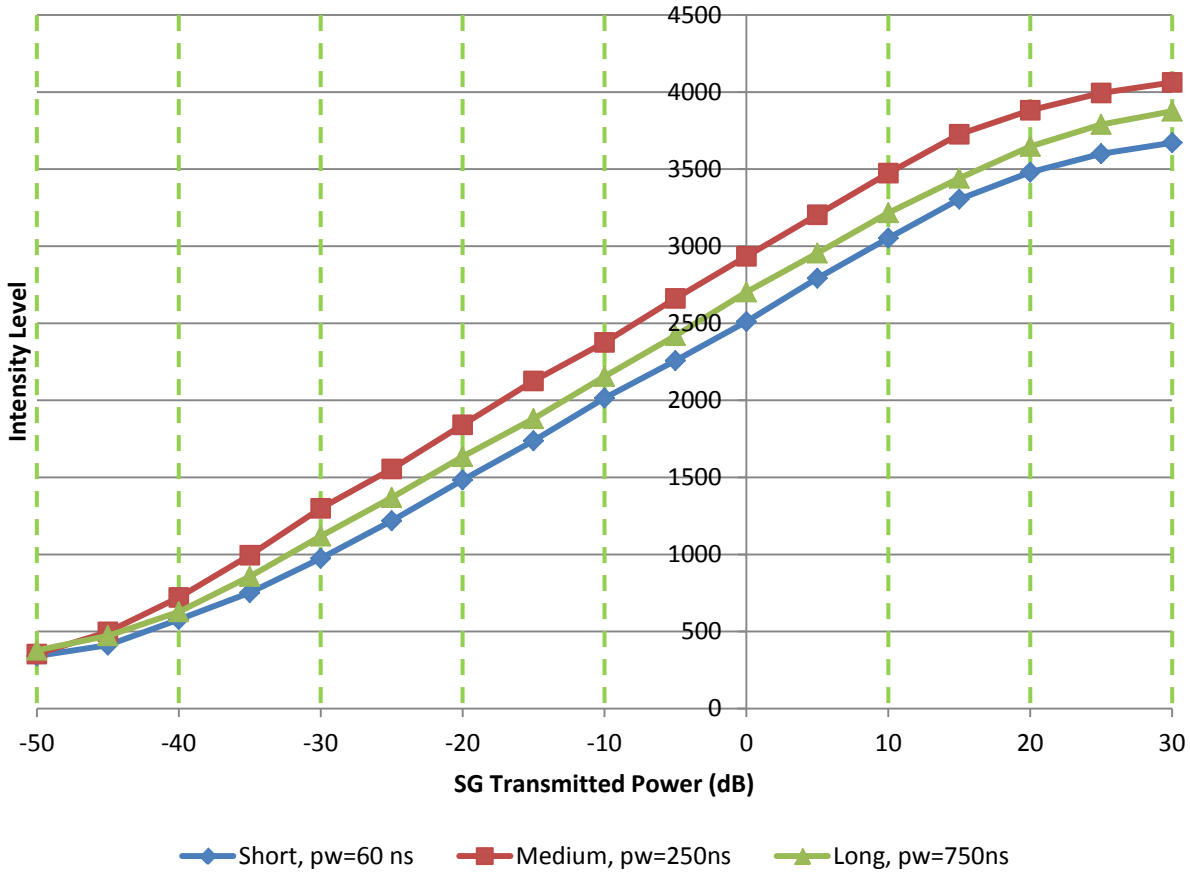

Figure 11: Consilium radar amplitude calibration curves, created by injecting signal generator pulses into the transceiver using a directional coupler.

Figure 12 shows the comparison between the results for Consilium radar obtained from first and third scenario. A very good agreement is observed. The analysis in the first scenario calculated the maximum intensity level over all the pixels along the main-beam azimuth-value and then median value is obtained over the number of scans (30 scans). In the third scenario, a pixel with a fixed location is chosen on the ring shown in Fig. 4. The intensity level is measured for each scan and the average value is calculated over 7 scans. Due to the different ways of analyzing the data the first scenario had a higher noise level than the third scenario and therefore data points could not be obtained below 720 intensity levels. The third scenario analysis allowed the data points to be seen down to a minimum of 350 intensity levels.

Fig. 13 shows the calibration curve obtained for the Consilium radar when the radar was set to short pulse, and the injected pulse had a pulse width of pw = 60 ns, and 1 μs.

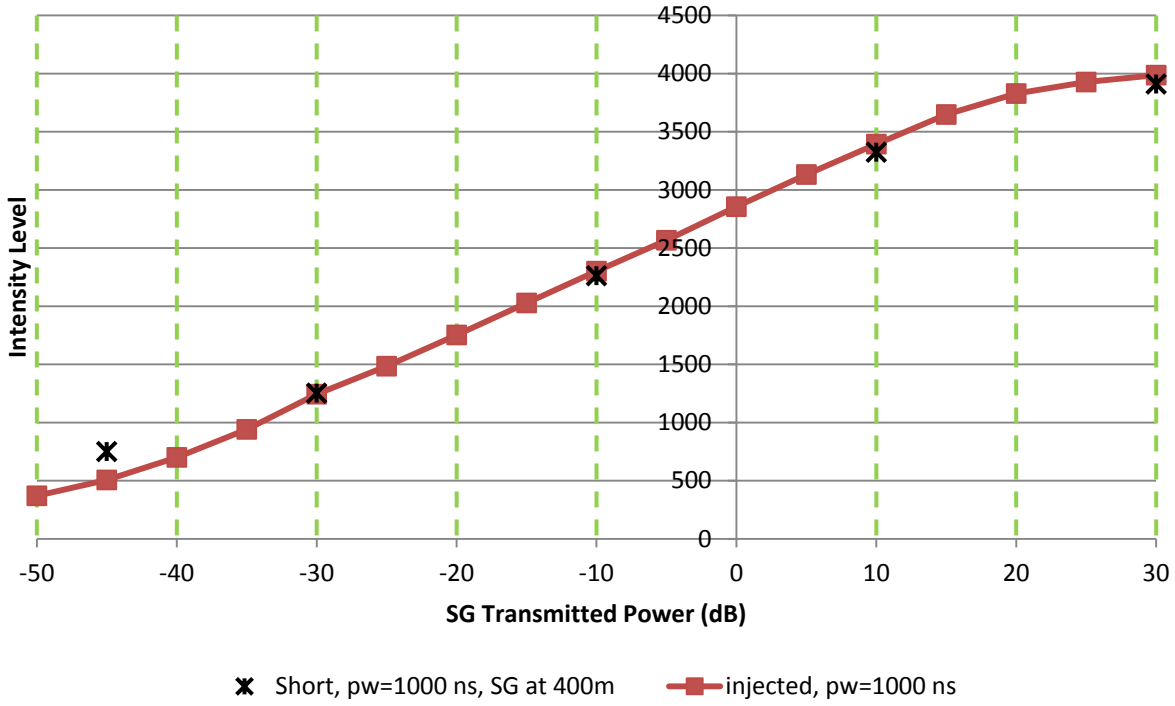

Figure 12: Comparison of the Consilium radar calibration curves obtained from the first scenario and the third scenario. The radar was set to short pulse during both recordings.

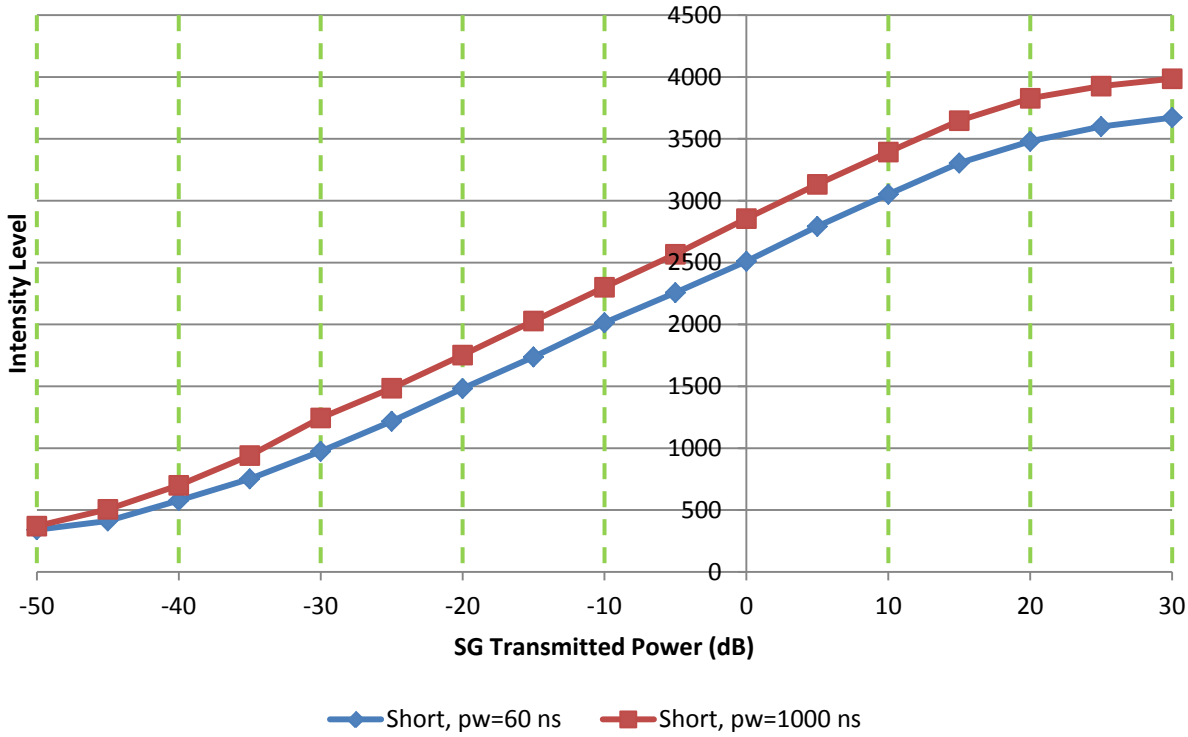

Figure 13: Comparison of the Consilium radar calibration curves obtained using the third scenario, with different injected pulse widths, with the radar set to short pulse.

A4. Final Calibration Curves

Fig. 14 shows the Consilium radar set up with the directional coupler placed at point A (point A is the power at the Signal Generator). The losses from point A to the transceiver include the SMA to N adaptor (-0.14 dB), the 10 dB attenuator (-9.96 dB), the 2 meter coax cable (-2.33 dB), the N to waveguide adaptor (-0.2 dB), and the directional couple loss (-39.3 dB). That gives a total loss from point A to the Transceiver input of -51.93 dB. The losses from point C to the transceiver include 0.5 m of elliptical waveguide which has a loss of 0.1 dB/m (total = 0.05 dB), two 90 degree bends which are -0.1 dB each (total = -0.2 dB), the turning unit rotary joint which is -0.5 dB, and the antenna gain of +31 dB. This means the received power at the transceiver is equal to the power at point C + 30.25 dB. Therefore the difference between the received power at point C and the injected power at point A can be determined by equating the above at the input to the transceiver as follows:

$$C + 30.25\ dB = A - 51.93\ dB \tag{1}$$

Therefore

$$C = A - 51.93\ dB - 30.25\ dB = A - 82.2\ dB \tag{2}$$

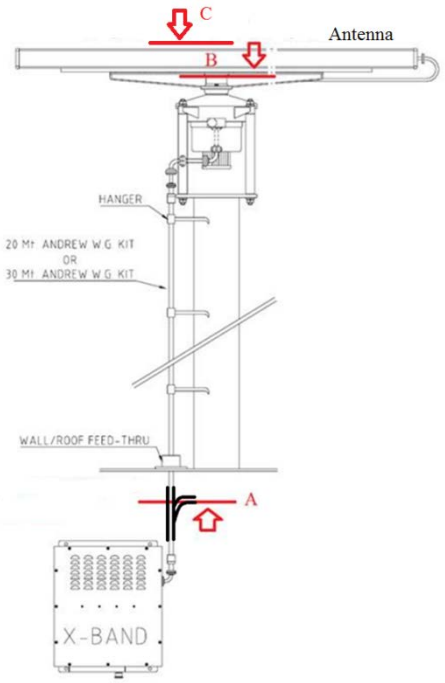

Figure 14: Consilium radar showing the location of the directional coupler.

The received power curve at point C versus the intensity level can be obtained using equation 2 and the data from figure 11. The results are shown in Table III.

Table III: Consilium Calibration Curve Data Relating Power Intensity at Point C to the Radar Intensity Level

dB level at Point A	dB level at Point C	Intensity level		
		Short	Medium	Long
	Noise Floor	327	337	317
-55	-137.2	328	358	359
-50	-132.2	362	383	378
-45	-127.2	399	489	472
-40	-122.2	541	738	628
-35	-117.2	740	1001	857
-30	-112.2	990	1286	1119
-25	-107.2	1235	1548	1368
-20	-102.2	1491	1842	1634
-15	-97.2	1742	2107	1880
-10	-92.2	2004	2368	2155
-5	-87.2	2264	2650	2420
0	-82.2	2533	2923	2703
5	-77.2	2800	3190	2955
10	-72.2	3056	3466	3217
15	-67.2	3296	3709	3441
20	-62.2	3490	3867	3647
25	-57.2	3610	3979	3790
30	-52.2	3683	4045	3875

In order to compare the results obtained in the second and third scenario, the results in table I are mapped to power levels using Table III (see table IV for results) and the expected received power at point C for the Luneburg lens was calculated using Carpet by setting the received power antenna gain, and signal processing losses to 0 dB. It is noted that the intensity level at 400 m (short pulse) is 3978, and it is out of the measurement range given in Table III. Assuming the magic number of 40, the extrapolated power level is -50 dB (corresponding to intensity level of 3978). The results of these two calculations (measured results vs. simulated) are shown in Figure 15. The agreement is satisfactory at 300 m and 400 m when the actual target height is used in Carpet modeling. However, the results do not agree for the target at 500 m. It is speculated that the difference is cause by the curved shape of the runway as Shown in Fig. 2. By changing the target height to 0.4 m (this is estimated from the pictures in Fig. 2(c) and because of curved runway), the agreement becomes satisfactory at 500 m.

Table IV: Power Intensity (dB) at Point C Obtained for the Lens Target

		300 m	400 m	500 m
Consilium	Short	-70.0	-50.0	-62.7
	Medium	-67.3	Saturated	-51.8
	Long	-64.6	Saturated	-51.9

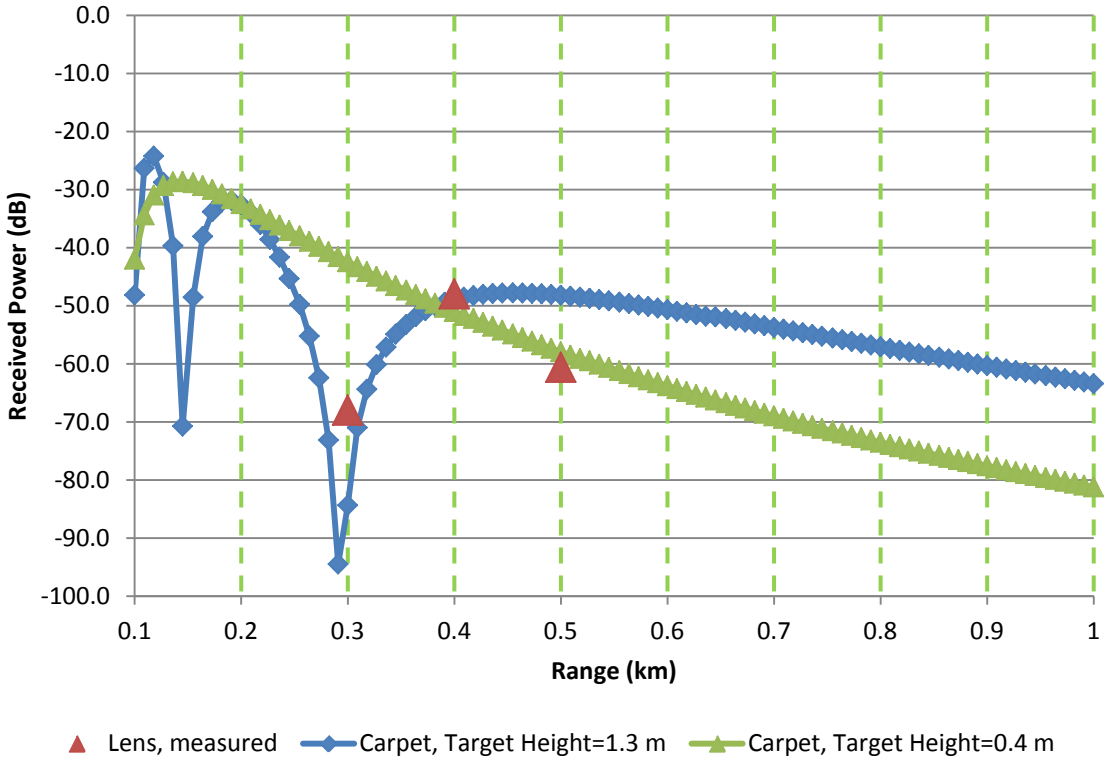

Figure 15: Carpet results showing the received power versus range with Consilium radar parameters and a lens as a target with RCS=10 m^2 (short pulse). The simulated results are compared with the measured values at Bell island. Two sets of Carpet simulations are needed (with target height of 0.4 and 1.3 m) to compensate the effect due to the runway curvature.

A Carpet model was then run for the Sperry radar in the second scenario. The simulation results show that the Sperry radar should have 0.5 dB less power at point C compared to the Consilium radar system. This difference is due to the Sperry transmit antenna gain being 0.5 dB lower than the Consilium transmit antenna gain. By using these simulation results and the results from the first scenario, the short-pulse calibration curve for the Sperry radar was derived and is shown in Table V and Fig. 16. This curve was derived using the curve obtained in first scenario and shifting it horizontally so that it crosses the intensity level of the 500 m target obtained in the second scenario. It is noted that the data point at 300 m is not reliable since it is close to a null point (very sensitive to the range). Furthermore, the data point at 400 m is not suitable for the calculation since it is close to the power level where the signal generator was almost saturated. The data point at 500 m was not sensitive to range and it was away from the SG saturation point. Fig. 17 compares the short-pulse calibration curves of the Sperry and Consilium radar systems.

Table V: Short Pulse Sperry Calibration Curve Data Relating Power Intensity at Point C to the Radar Intensity Level

dB level at Point C	Intensity Level Short Pulse
-44.4	3765
-49.4	3707
-54.4	3491
-59.4	3260
-64.4	3047
-69.4	2761
-74.4	2566
-79.4	2323
-84.4	2092
-89.4	1876
-94.4	1611
-99.4	1429
-104.4	1183
-109.4	1008
-114.4	937

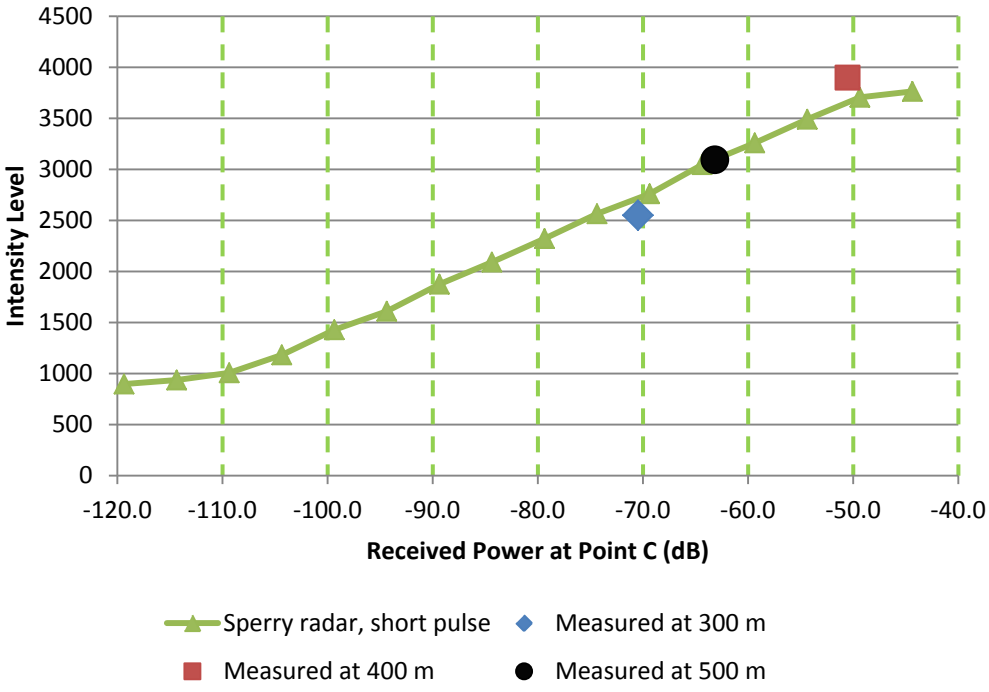

Figure 16: Sperry calibration curve for short pulse, relating power intensity at point C to the radar intensity level.

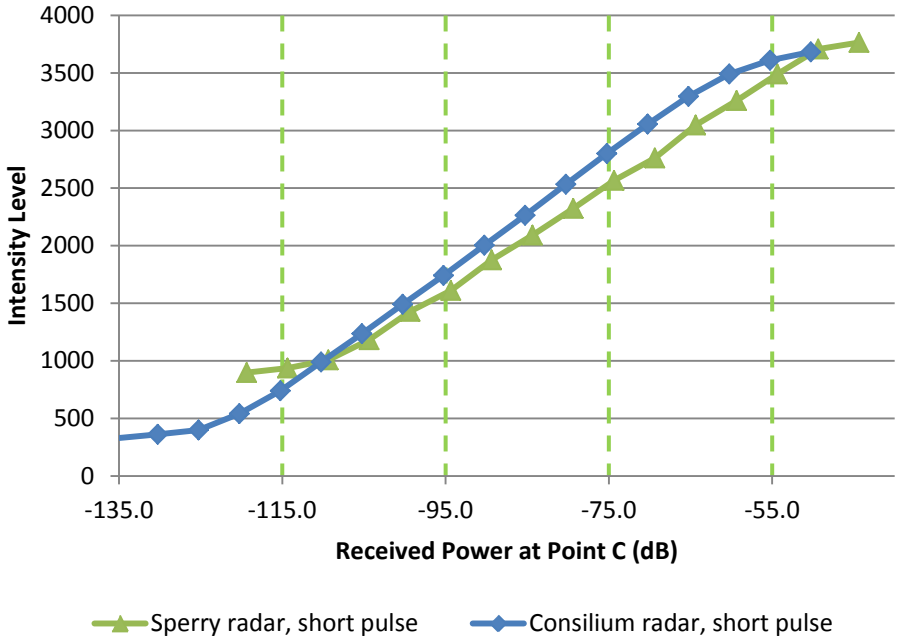

Figure 17: Comparing the short-pulse calibration curves obtained for two radar systems.

The medium and long pulse calibration curves for the Sperry were derived in the same way as for short pulse and are shown in Table VI and Table VII and Fig. 18 and Fig. 20. The intensity level for the target at 500 m in the second scenario is used as a fix point with the slope obtained from the first scenario. Fig. 19 and Fig. 21 compare the medium and long pulse calibration curves of the Sperry and Consilium radar systems.

Table VI: Medium Pulse Sperry Calibration Curve Data Relating Power Intensity at Point C to the Radar Intensity Level

dB level at Point C	Intensity Level Medium Pulse
-39.3	3731
-44.3	3705
-49.3	3493
-54.3	3264
-59.3	3039
-64.3	2761
-69.3	2579
-74.3	2322
-79.3	2093
-84.3	1882
-89.3	1604
-94.3	1431
-99.3	1196
-104.3	1003
-109.3	927

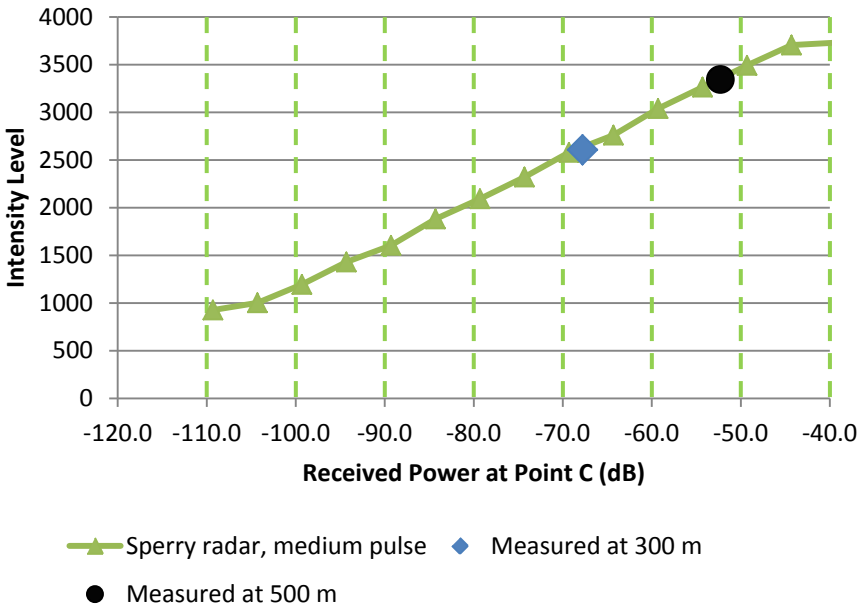

Figure 18: Sperry calibration curve for medium pulse, relating power intensity at point C to the radar intensity level.

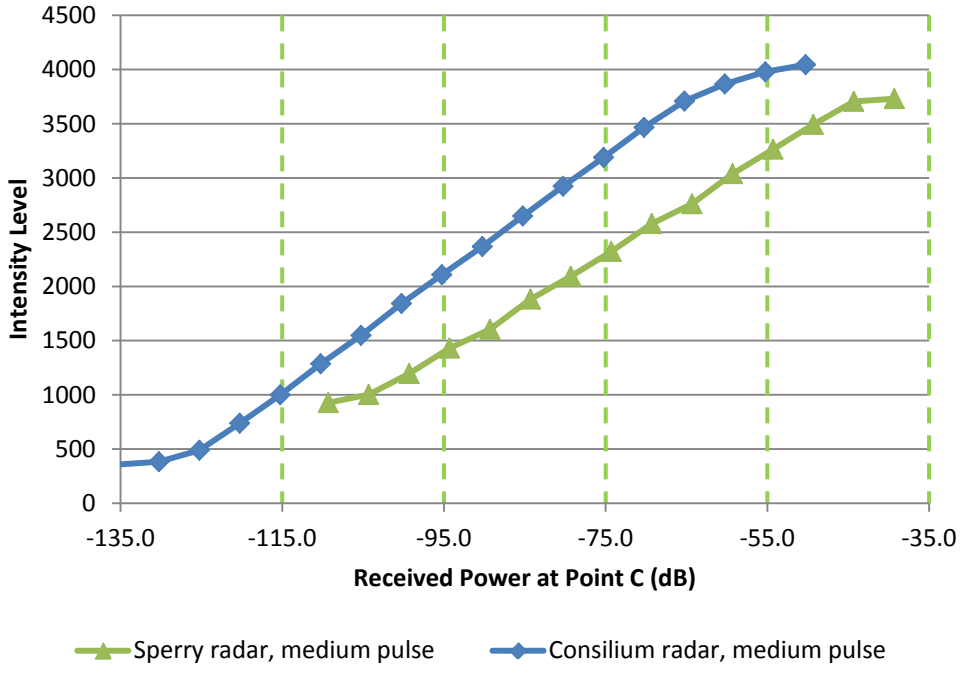

Figure 19: Comparing the medium-pulse calibration curves obtained for two radar systems.

Table VII: Long Pulse Sperry Calibration Curve Data Relating Power Intensity at Point C to the Radar Intensity Level

dB level at Point C	Intensity Level Long Pulse
-40.5	3797
-45.5	3790
-50.5	3561
-55.5	3336
-60.5	3116
-65.5	2875
-70.5	2645
-75.5	2468
-80.5	2181
-85.5	2005
-90.5	1753
-95.5	1543
-100.5	1375
-105.5	1138
-110.5	985

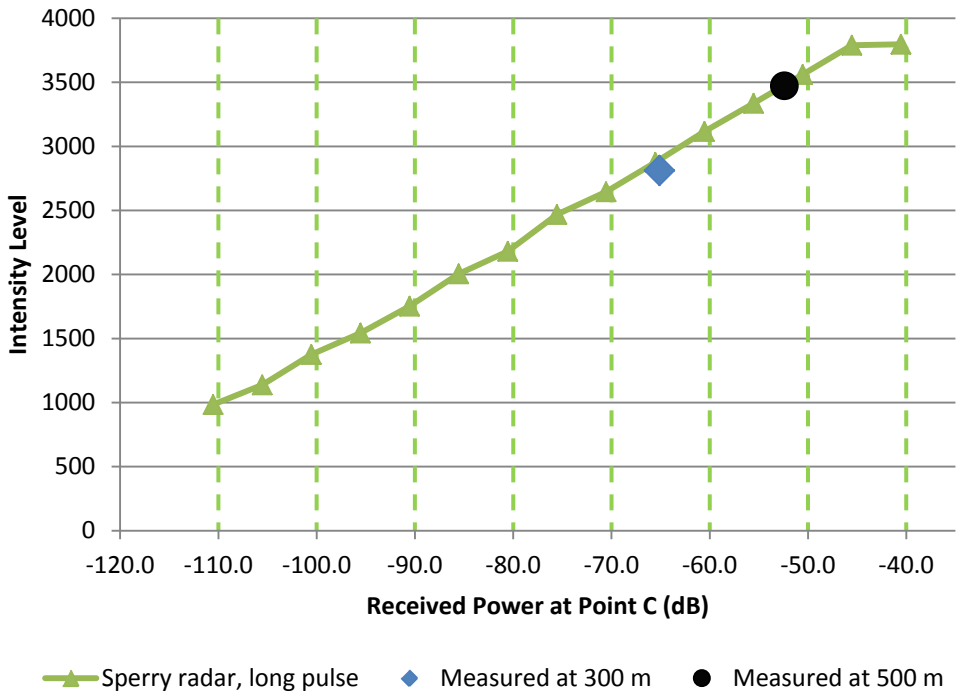

Figure 20: Comparing the long-pulse calibration curves obtained for two radar systems.

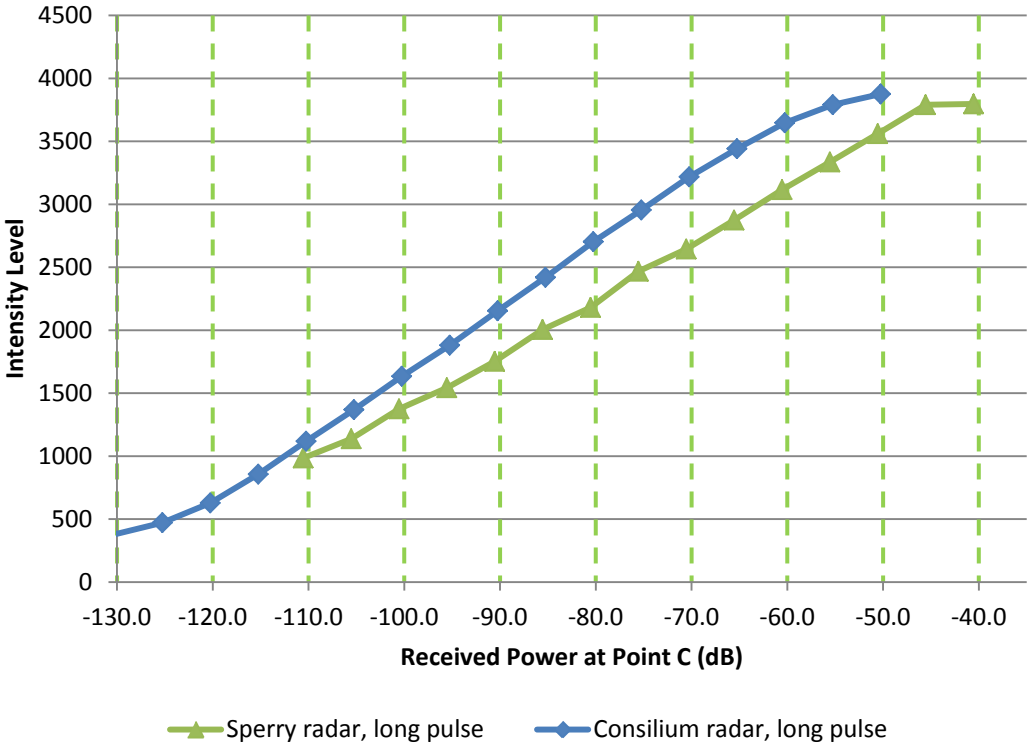

Figure 21: Comparing the long-pulse calibration curves obtained for two radar systems.

Appendix B: Transmitted Pulse Parameters (Consilium Radar Only)

This appendix shows the measured transmitted pulse parameters for Consilium radar.

Transmit Calibration

Day	Short	Medium	Long
Dec 08	▲T: 80ns AVG: 1.60dBm Peak: 3.50dBm PK-AVG: 1.90	▲T: 284ns AVG: 2.45dBm Peak: 3.90dBm PK-AVG: 1.40db	
Dec 14	▲T:82.6ns AVG: 1.4dBm Peak: 3.60dBm PK-AVG: 2.18	▲T: 248ns AVG: 2.60 Peak: 4.00 PK-AVG 1.40	
Dec 17	▲T: 78.3ns AVG: 1.58dBm Peak: 3.45dBm PK-AVG 1.90db	▲T: 248ns AVG 2.45dBm Peak: 3.85dBm PK-AVG 1.40	
Dec 29	▲T:78.3ns AVG 1.72dBm Peak: 3.60dBm PK-AVG 1.90db	▲T:101ns AVG 2.9dBm Peak: 4.0dBm PK-AVG 1.20dBm	
Jan 03	▲T:80.0ns AVG 1.65dBm Peak: 3.6dBm PK-AVG 1.90db	▲T:248ns AVG 2.51dBm Peak: 4.0dBm PK-AVG 1.50dBm	
Jan 05	▲T: 82.6ns AVG: 1.66dBm Peak: 3.60dBm PK-AVG: 1.90	▲T: 248ns AVG: 2.58dBm Peak: 4.01dBm PK-AVG: 1.56db	
Jan 18	▲T: 82.6ns AVG: 1.67dBm Peak: 3.65dBm PK-AVG: 1.90db	▲T: 248ns AVG: 2.60dBm Peak: 4.10dBm PK-AVG: 1.50db	▲T: 757ns AVG: 2.62dBm Peak: 4.15dBm PK-AVG: 1.50db
Jan 26	▲T: 80ns AVG: 1.71dBm Peak: 3.70dBm PK-AVG: 1.95db		

▲T: Pulse Width
AVG: Average Amplitude
Peak: Peak Amplitude

Note: 10db and 20db attenuators were used on all transmit calibrations

Appendix C: Glossary

Blob	A bright spot on the radar screen which represent the location of the target or clutter.
B-Scan	B-scan is a two dimensional display of the area around the radar platform. The horizontal and vertical axes usually represent the range and bearing. The returned signals from the targets are displayed with a bright color on the screen**.**
Radar Resolution Cell	Radar resolution cell is the smallest area of the radar image that can be resolved and is a function of antenna beam width, pulse length and range**.**